Determining Soil Volumetric Moisture Content Using Time Domain Reflectometry

ROAD
TEST
151008

U.S. Department of Transportation
Federal Highway Administration

Research and Development
Turner-Fairbank Highway Research Center
6300 Georgetown Pike
McLean, VA 22101-2296

LTPP

FOREWORD

Determining the moisture content of pavement structures for seasonal variations has long been a key concern for pavement designers. Until now, estimates or "best guess" moisture levels provided the basis for design parameters. Today, through the use of Time Domain Reflectometry, moisture content can be calculated accurately and inexpensively.

This document provides information to pavement engineers on Time Domain Reflectometry, a technique that indirectly measures the in situ volumetric moisture content of soil. It describes the technique and presents a model for predicting volumetric moisture content.

The Federal Highway Administration (FHWA) has distributed this document primarily in electronic form. Copies are being sent to FHWA regional and division offices, Strategic Highway Research Program Coordinators, and all data users. A copy can be found through the LTPP web page at http://www.tfhrc.gov/pavement/ltpp/ltpphome.htm by selecting the LTPP Data Base button.

Charles J. Nemmers, P.E.
Office of Engineering
Research and Development

NOTICE

This document is distributed under the sponsorship of the Department of Transportation in the interest of information exchange. The United States Government assumes no liability for its contents or use thereof. This report does not constitute a standard, specification, or regulation.

The United States Government does not endorse products or manufacturers. Trade and manufacturers' names appear in this report only because they are considered essential to the object of the document.

1. Report No. FHWA-RD-97-139	2. Government Accession No.	3. Recipient's Catalog No.	
4. Title and Subtitle DETERMINING SOIL VOLUMETRIC MOISTURE CONTENT USING TIME DOMAIN REFLECTOMETRY		5. Report Date February 1998	
		6. Performing Organization Code	
7. Author(s) John Klemunes, Jr.		8. Performing Organization Report No.	
9. Performing Organization Name and Address Office of Engineering R&D Federal Highway Administration 6300 Georgetown Pike McLean, VA 22101-2296		10. Work Unit No. (TRAIS) 3C6a	
		11. Contract or Grant No.	
12. Sponsoring Agency Name and Address Office of Engineering R&D Federal Highway Administration 6300 Georgetown Pike McLean, VA 22101-2296		13. Type of Report and Period Covered Final Report June 1994 - December 1995	
		14. Sponsoring Agency Code	
15. Supplementary Notes Contracting Officer's Technical Representative (COTR): Shahed Rowshan, HNR-30			

16. Abstract

Time domain reflectometry (TDR) is a technique used to measure indirectly the in situ volumetric moisture content of soil. Current research provides a variety of prediction equations that estimate the volumetric moisture content using the dielectric constant calculated from the apparent length obtained from the TDR reader. However, very limited research exists regarding which of several available procedures should be used to obtain the apparent length of the TDR response for use in calculating the dielectric constant.

The purpose of this study is to enhance the predictive accuracy of in situ volumetric moisture content estimation from TDR measurements. The study is divided into two phases. The initial phase evaluates the five known methods of analyzing the apparent length of TDR responses to determine which provides the most accurate method for estimating the volumetric moisture content.

Phase II, through a mixing model form, regresses the volumetric properties of the soil and the apparent length of the TDR response to obtain a predicted volumetric moisture content.

17. Key Words Volumetric moisture, dielectric constant, time domain reflectometry.		18. Distribution Statement No restrictions. This document is available to the public through the National Technical Information Service, Springfield, VA 22161.	
19. Security Classif. (of this report) Unclassified	20. Security Classif. (of this page) Unclassified	21. No. of Pages 74	22. Price

Form DOT F 1700.7 (8-72)　　Reproduction of completed page authorized

This form was electronically produced by Elite Federal Forms, Inc.

SI* (MODERN METRIC) CONVERSION FACTORS

APPROXIMATE CONVERSIONS TO SI UNITS

Symbol	When You Know	Multiply By	To Find	Symbol
LENGTH				
in	inches	25.4	millimeters	mm
ft	feet	0.305	meters	m
yd	yards	0.914	meters	m
mi	miles	1.61	kilometers	km
AREA				
in²	square inches	645.2	square millimeters	mm²
ft²	square feet	0.093	square meters	m²
yd²	square yards	0.836	square meters	m²
ac	acres	0.405	hectares	ha
mi²	square miles	2.59	square kilometers	km²
VOLUME				
fl oz	fluid ounces	29.57	milliliters	mL
gal	gallons	3.785	liters	L
ft³	cubic feet	0.028	cubic meters	m³
yd³	cubic yards	0.765	cubic meters	m³

NOTE: Volumes greater than 1000 l shall be shown in m³.

Symbol	When You Know	Multiply By	To Find	Symbol
MASS				
oz	ounces	28.35	grams	g
lb	pounds	0.454	kilograms	kg
T	short tons (2000 lb)	0.907	megagrams (or "metric ton")	Mg (or "t")
TEMPERATURE (exact)				
°F	Fahrenheit temperature	5(F-32)/9 or (F-32)/1.8	Celcius temperature	°C
ILLUMINATION				
fc	foot-candles	10.76	lux	lx
fl	foot-Lamberts	3.426	candela/m²	cd/m²
FORCE and PRESSURE or STRESS				
lbf	poundforce	4.45	newtons	N
lbf/in²	poundforce per square inch	6.89	kilopascals	kPa

APPROXIMATE CONVERSIONS FROM SI UNITS

Symbol	When You Know	Multiply By	To Find	Symbol
LENGTH				
mm	millimeters	0.039	inches	in
m	meters	3.28	feet	ft
m	meters	1.09	yards	yd
km	kilometers	0.621	miles	mi
AREA				
mm²	square millimeters	0.0016	square inches	in²
m²	square meters	10.764	square feet	ft²
m²	square meters	1.195	square yards	yd²
ha	hectares	2.47	acres	ac
km²	square kilometers	0.386	square miles	mi²
VOLUME				
mL	milliliters	0.034	fluid ounces	fl oz
L	liters	0.264	gallons	gal
m³	cubic meters	35.71	cubic feet	ft³
m³	cubic meters	1.307	cubic yards	yd³
MASS				
g	grams	0.035	ounces	oz
kg	kilograms	2.202	pounds	lb
Mg (or "t")	megagrams (or "metric ton")	1.103	short tons (2000 lb)	T
TEMPERATURE (exact)				
°C	Celcius temperature	1.8C + 32	Fahrenheit temperature	°F
ILLUMINATION				
lx	lux	0.0929	foot-candles	fc
cd/m²	candela/m²	0.2919	foot-Lamberts	fl
FORCE and PRESSURE or STRESS				
N	newtons	0.225	poundforce	lbf
kPa	kilopascals	0.145	poundforce per square inch	lbf/in²

* SI is the symbol for the International System of Units. Appropriate rounding should be made to comply with Section 4 of ASTM E380.

(Revised September 1993)

TABLE OF CONTENTS

LIST OF FIGURES

LIST OF TABLES

CHAPTER I: INTRODUCTION

The Long-Term Pavement Performance (LTPP) study's Seasonal Monitoring Program (SMP) was intended to provide: (1) the means to link the pavement response data obtained at random points in time to critical design conditions; (2) the means to validate models for relationships between environmental conditions and in situ properties of pavement material; and (3) new knowledge of the magnitude and impact of the changes involved (19).

One component of this program involved the in situ measurement of moisture content in the pavement system. For this measurement technique, the dielectric properties of the pavement layer were selected as affording the best solution methodology. To this end, pilot studies used time domain reflectometry (TDR) and frequency shift resonant circuit measurement systems. The major recommendation from the pilot field trials was that the TDR procedure was superior and was hence incorporated into the program.

Based on these efforts, the Federal Highway Administration (FHWA) initiated a study to enhance the predictive accuracy of in situ volumetric moisture content estimation from TDR measurements. Specifically, current TDR research provides a range of prediction equations to estimate the volumetric moisture content of soil. These equations calculate the dielectric constant using the apparent length of the TDR response. There are, however, five known methods for determining the apparent length of the TDR response. Limited research has been undertaken to determine which method provides the most accurate results and hence the most reliable predictive equation.

Phase I of this study evaluates the five known methods of analyzing the apparent length of TDR response to determine which provides the most accurate results. Phase II builds on the Phase I results, developing a series of hierarchical models that can be used to estimate volumetric moisture in highway soils based on a knowledge of the soil properties.

STUDY OBJECTIVES

The objectives of this study are: to determine the most accurate procedure for establishing the apparent length (L_a), and hence the dielectric constant, of the TDR signal response on a soil mixture; and, to develop an improved multiple-regression model to estimate the volumetric moisture content in highway soils.

CHAPTER II: LITERATURE REVIEW

TIME DOMAIN REFLECTOMETRY BACKGROUND

Time domain reflectometry (TDR) was originally developed to detect breaks in communication cables. In the 1950s, it was adopted by the agricultural community to measure soil moisture. The principle of the TDR system is similar to that of a radar system. An electromagnetic waveform is transmitted through a medium, and any obstruction or change in impedance sends a portion of the reflected waveform back to the source (19).

Unbound materials used in pavement structures are comprised of a three-phase system: soil solids, air, and water (24). The dielectric constant[1] for air is 1. For most minerals comprising soil and aggregate systems, the dielectric constant typically varies between 3 and 5, while the dielectric constant of water is typically near 80 (4,13). As water has such a large dielectric constant (compared to the air and solid phases), the amount of water present in a soil-water-air mixture is the primary determinant of the dielectric constant of the mixture between the conducting surfaces of a TDR probe. For a completely dry soil, the composite dielectric constant will be slightly less than the dielectric constant for the soil solids. As moisture is added to the soil, the composite dielectric constant increases due to the large dielectric constant of water.

To measure soil moisture using the TDR approach, a Tektronix 1502B cable tester is used to emit an electromagnetic pulse throughout a coaxial cable connected to the TDR probe. The electromagnetic pulse travels through the center of the coaxial cable at approximately the speed of light, factored by the resistance of the cable in air, and then through the center rod of the TDR probe. Once the pulse reaches the end of the probe, a portion of the signal is reflected back through the shielding of the coaxial cable to the Tektronix unit. The reflected voltage versus time is registered on a screen display of the Tektronix unit and/or saved to an ASCII file. The portion of the trace of interest goes from when the signal reaches the beginning of the probe to the point when the signal reaches

---

[1] A dielectric is defined as an insulating medium between two plates of a capacitor. The dielectric constant of a specific material is defined as the ratio of the capacitance of that material to the capacitance of air.

the end of the probe. A drop in reflected voltage is seen on the display of the Tektronix unit when the signal reaches the beginning of the TDR probe, due to the increased resistance of the smaller path in the printed circuit board, and a vast rise in the reflected voltage is noticed when the signal reaches the end of the probe (20).

The TDR probe has a certain region of influence that is based on the probe design. A practical design for a TDR probe allows for the best resolution. Research has shown that the soil moisture measured by TDR has an area of influence in the shape of a cylinder whose axis lies midway between the rods and whose diameter is 1.4 times the spacing between the rods (2). Knight presented a theoretical investigation of the area of influence (23). He recommended that the area of influence is cylindrical and the probe be designed so that the ratio of the rod diameter divided by the spacing of the prongs be greater than 0.1, to insure that energy is not concentrated too closely around the rods (23).

The horizontal distance between the initial and final inflection points of the TDR trace response, as measured by an oscilloscope, is the travel time of the signal. This travel time represents the apparent length (L_a) of the TDR response. Knowledge of the actual probe length and signal speed permits a calculation of an "apparent dielectric constant" (K_a) of the media into which the TDR probe is inserted.

In reality, the dielectric constant is a complex number containing both a real and animaginary part of the electrical loss (6). However, over a frequency of 1 MHZ to 1 GHz, the real part of the dielectric constant does not exert a strong influence. For soils studied to date, electrical loss is small and does not significantly alter the measured propagation velocity (6). As a consequence, the computed dielectric constant is referred to as the "apparent dielectric constant" (K_a) and is defined by equation 1.

$$K_a = [\frac{(L_a)}{(L)(V_p)}]^2 = [\frac{(B - A)}{(L)(V_p)}]^2 \tag{1}$$

where: K_a = dielectric constant.
                L_a = $(B - A)$ = apparent length of probe (m).
                           B = final inflection point.
                           A = initial inflection point.
                L = actual length of probe (m); 0.203 m for FHWA probes.
                V_p = the ratio of the actual propagation velocity to the speed of light; on TDR cable tester, the phase velocity setting (usually 0.99 for maximum resolution).

Once the K_a is computed for a specific soil mixture, a correlation equation is used to predict the volumetric moisture content.

TDR RESPONSE FACTORS

Although the theoretical basis for correlating the apparent dielectric constant K_a, to volumetric moisture content is fundamentally sound, a variety of practical considerations influence the K_a value. These factors include:

- Analysis methodology for establishing L_a (apparent length).
- Soil mineral dielectric constant variability.
- Water dielectric constant variability:
    - Free versus bound water.
    - Temperature effects.
    - Salinity.

Few studies have been done to determine the best methodology for establishing the apparent length of the TDR response and to factor in the variation present in repeating the TDR response readings (i.e., the response readings must fill the entire screen in the cable reader to obtain the highest possible resolution). Research has demonstrated that four consecutive readings of the same TDR response with improper resolution settings may produce a variation of 6 percent absolute error in volumetric moisture content (4).

The five known methods of determining the apparent length of the TDR trace are: Method of Tangents (1,5,6); Method of Peaks (1,15); Alternate Method of Tangents (1); Method of Diverging Lines (1); and Campbell Scientific Method (25). Each method uses a slightly different location to measure the initial and final inflection points of the trace signal.

5

The Method of Tangents and Method of Peaks are widely used by researchers today. The Campbell Scientific Method was developed by Campbell Scientific and is used in their data loggers for recording seasonal variations (however, no research has been found to determine the validity of this method). These three methods have worked well for studies, as the interpretation of their results is relatively easy and repeatable compared to the Alternate Method of Tangents and the Method of Diverging Lines. However, using these three methods, it is difficult to determine the final inflection point for many TDR response traces, due to the manner in which the final inflection point is determined. (Interpretation of the TDR response is covered in greater detail in an ensuing chapter of this report.) Although the Method of Tangents, Method of Peaks, and Campbell Scientific Method are still in use today, there is little if any justification for using them.

Another key factor that influences the dielectric constant is soil mineral dielectric constant variability. Generally, fine- and coarse-grained soils have distinctly different mineral compositions. Fine-grained soils are primarily comprised of magnesium and calcium, while coarse-grained soils predominately contain silica and quartz. This difference in general mineral types may produce a large variation in dielectric values. The dielectric constant of minerals present in fine-grained soils is approximately 4, while coarse-grained soils have a dielectric constant in the range of 8; however, very little research on this variability has been conducted (26).

The water constant variability factor includes the influence of free versus bound water in the soil. Water's chemical composition affects the dielectric constant because absorbed (bound) water has a much lower dielectric constant than free pore water (13). For saturated versus partially saturated soils, the soil volumetric moisture content is the predominant factor in determining the relative dielectric constant (4,5). Most predictive moisture equations use the dielectric constant as a predictor variable to determine the volumetric moisture content. When volumetric moisture content falls below 5 percent, the dielectric constant is increasingly influenced by the soil type and mineralogy (4,6). When this condition occurs, three parameters must be determined more accurately: the composite dielectric number, the dielectric number of the soil matrix, and the porosity (6).

There are mixed opinions regarding the influence of the temperature factor on the dielectric constant. Some researchers have determined that temperatures ranging from 0 to 25° C have "minimal" effect on the soil's dielectric constant (4). Topp has shown that the variation from 10 to 35° C is less than the experimental error of $\pm$ 1 K_a at T = 20.5° C (5). On the other hand, some researchers have determined that temperatures ranging from 0 to 25° C have a significant effect on the soil's dielectric constant (13, 19). Such research has found that with higher levels of moisture, higher frequencies (50 MHz to 10 GHz), and different modes of the electromagnetic field, temperature becomes more important (6). The dielectric constant decreases rapidly over the temperature range of 0 to -1.0° C, with a decreasing rate of change at lower temperatures (11). Temperature effects may be neglected for fluctuations of $\pm$5° C and depths greater than 0.5 m. A simple linear correction is required for temperatures exceeding this fluctuation (4).

Saline conditions are another key factor in establishing the dielectric constant and are difficult to determine using the TDR. This is due to the imaginary portion of the complex dielectric constant. Remember that the apparent dielectric constant used in TDR assumes the imaginary portion is insignificant (6). Topp has shown that when salt is added to the sample, more scatter is found in the relationship between V_w (volumetric moisture content) and K_a (5). When a saline solution is present in the area where the TDR probe is located, a short-circuiting occurs to the probe, making the final inflection point of the TDR response difficult to interpret (16). Research has shown that the dielectric is less affected by salt concentration than measurements by conductivity methods. The shape of the calibration curve changes with increased salt concentrations (4). Frequency domain has been used to account for the amount of salinity present (24).

EXISTING MODEL FORMS

In general, researchers have relied upon two different approaches to relate soil volumetric moisture content to the dielectric constant using the TDR response. The first approach selects functional relationships purely by their mathematical flexibility in fitting the experimental data points. No attempt is made to give a physical or rational scientific justification to the model. Below the relaxation frequency of water, a relationship between the dielectric number and the volumetric moisture content of the soil is determined using a

third-order polynomial (6). Topp was one of the first researchers who determined this third-order polynomial relationship (5). His equation has the functional form of equation 2.

$$Q = -5.3 \times 10^{-2} + 2.92 \times 10^{-2}K_a - 5.5 \times 10^{-4}K_a^2 + 4.3 \times 10^{-6}K_a^3 \qquad (2)$$

where: Q = volumetric moisture content.
             K_a = dielectric constant.

Since this initial estimate, other researchers such as Paterson and Roth, have used this same functional form with other constants to estimate the soils tested, with better results (14). The major advantage of this model form is that no gravimetric or volumetric soil properties are required. However, the accuracy of this model form has not been proven for all soils, especially fine-grained ones (6). Most studies using this third-order polynomial use a fixed volume mold, with a known water content added. This test method allows the researcher to predict the dielectric constant with a known volumetric moisture content (5,16).

A more suitable equation for a granular material is (16):

$$K_a = 3.91 + 30.1V_w + 198.8V_w^2 - 417.3V_w^3 \qquad (3)$$

where: V_w = volumetric moisture content.
(Note: The variables V_w and Q, as used throughout this study, are synonymous.)

This is then solved for the volumetric moisture content using the measured dielectric values. However, this is a statistically invalid process, since the deviations in the ordinate and abscissa are assumed equal.

In the second approach, the fundamental equation is derived from dielectric mixing models, which relate the composite dielectric number of a multiphase mixture to the dielectric numbers and the volume fractions of its constituents. In the mixing law approach, the soil is considered to be a mixture of soil, water, and air. In addition, the mixing law may be extended to either a three- or four-phase system (5,6).

A three-phase system includes the porosity, K_a (dielectric component of the soil-water-air mixture), K_{bw} (dielectric component of the bound water = 3.2), K_a (dielectric component of air = 1), K_s (dielectric component of the solid = 3.5), and an alpha exponent raised to each dielectric value (= 0.5 to 0.81) (21). This alpha exponent is a geometric factor that depends on the spatial arrangement of the mixture and its orientation in the electric field (24). A four-phase model includes the combination of the variables in the three-phase model in addition to K_{fw} (dielectric component of the free water = 81) (21).

Many empirical and mixing model equations have been developed with a similar model form. In order to increase the prediction capabilities of a specific model form, tests must be run on specific soil samples. These tests would insure sound prediction capabilities for the volumetric moisture content. Tables 1a and 1b summarize many of the most popular empirical and mixing models available for use today. Common terms used in these tables are:

K_a = apparent dielectric number.

e_s = dielectric constant of the soil.

e_a = dielectric constant of the air.

e_w = dielectric constant of the water.

Q = volumetric moisture content.

Q_{bw} = $dp_b S$ where:

                  d = thickness 3×10^{-8} cm.

                  p_b = dry bulk density.

                  S = specific surface area.

f = porosity.

a = alpha exponent, a geometric factor that depends on the spatial arrangement of the mixture and its orientation in the electric field.

bw = bound water.

fw = free water.

9

Table 1a. Existing Empirical Models.

1. Topp et al., 1980	$q = (A + B*K_a + C*K_a^2 + D*K_a^3) *10^{-4}$ $A = -530, B = 292, C = -5.5, D = 0.043$ (4 mineral soils)
2. Nadler et al., 1991	$A = -725, B = 367, C = -12.3, D = 0.150$ (silty loam)
3. Roth et al., 1992	$A = -728, B = 448, C = -19.5, D = 0.361$ (9 mineral) $A = -233, B = 285, C = -4.3, D = 0.030$ (7 organic)
4. Dasberg & Hopmans, 1992	$A = -751, B = 424, C = -18.5, D = 0.380$ (sandy loam) $A = -1096, B = 581, C = -22.7, D = 0.320$ (clay loam)
5. Jacobsen & Schjonning, 1993a	$A = -701, B = 347, C = -11.6, D = 0.180$ (10 mineral)
6. Maliki & Skierucha, 1989	$q = -19 + SQRT(388K_a - 546.9)/194, K_a \geq 1.41$ (5 mineral)
7. Ledieu et al., 1986	$q = 0.1138SQRT(K_a) - 0.1758$ $q = 0.1138SQRT(K_a) - 3.38p_b - 0.1529$ (mineral soil)
9. Jacobsen & Schjonning, 1993a	$q = (-341 + 345K_a - 11.4K_a^2 + 0.171K_a^3 - 370p_b +$ (7.36% Clay + 47.7% org. mat) x 10^{-4} (10 mineral)

10

Table 1b. Existing Mixing Models.

Three-Phase Model	$Q = [K_a{}^a - (1 - f)e_s{}^a - fe_a{}^a]/(e_w{}^a - e_a{}^a)$
1. Roth et al., 1990	$a = 0.50$ (11 mineral and 2 organic soils)
2. "a" fitted to data from Jacobsen & Schjonning	$a = 0.66$ (10 mineral soils)
Four-Phase Model	$Q = K_a{}^a - Q_{bw}(e_{bw}{}^a - a_{fw}{}^a) - (1 - f)e_s{}^a - fe_a{}^a/(e_w{}^a - e_a{}^a)$, $Q > Q_{bw}$
1. Dirksen & Dasberg, 1993	$a = 0.49, 0.50, 0.52, 0.54, 0.60, 0.61, 0.81$ (8 mineral soils)
2. "a" fitted to data from Jacobsen & Schjonning	$a = 0.70$ (10 mineral soils)

CHAPTER III: LABORATORY PROCEDURE

LABORATORY EQUIPMENT

Three key pieces of equipment were used in the experimental study to obtain the laboratory TDR response: a Tektronix 1502C cable reader, the FHWA design TDR moisture probe (see figure 1), and a personal computer for data collection.

The Tektronix 1502C time domain reflectometer is a short-range metallic cable tester capable of detecting any changes in impedance throughout the cable and probe. The 1502C consists of a pulse generator that produces a fast-risetime step voltage, a sampler which transforms a high-frequency signal into a lower frequency output, and an oscilloscope or other display or recording device (3). The 1502C sends an electrical pulse down the cable. Since the unit is sensitive to impedance changes, the 1502C displays "hills and valleys" in the reflected pulse, thereby detecting any reflections made by discontinuities.

There are many controls on the Tektronix 1502C, but most remain constant throughout the testing operation. If the displayed waveform contains noise, the apparent noise can be reduced by averaging. The filter settings range from 1 to 128 sample averages per trace. When the 128 setting is chosen, the 1502C will take the average of the128 signals and display this average trace on the screen. (FHWA has decided to use the 128 setting since many external sources influence the TDR trace stability.)

The horizontal scale is another setting held constant. The DIST/DIV scale determines the number of meters per division across the display. A constant setting of 0.25 m per division is used to fit the entire 251-point waveform in the display and achieve the best resolution. The trace interpretation is easier when this setting is held constant.
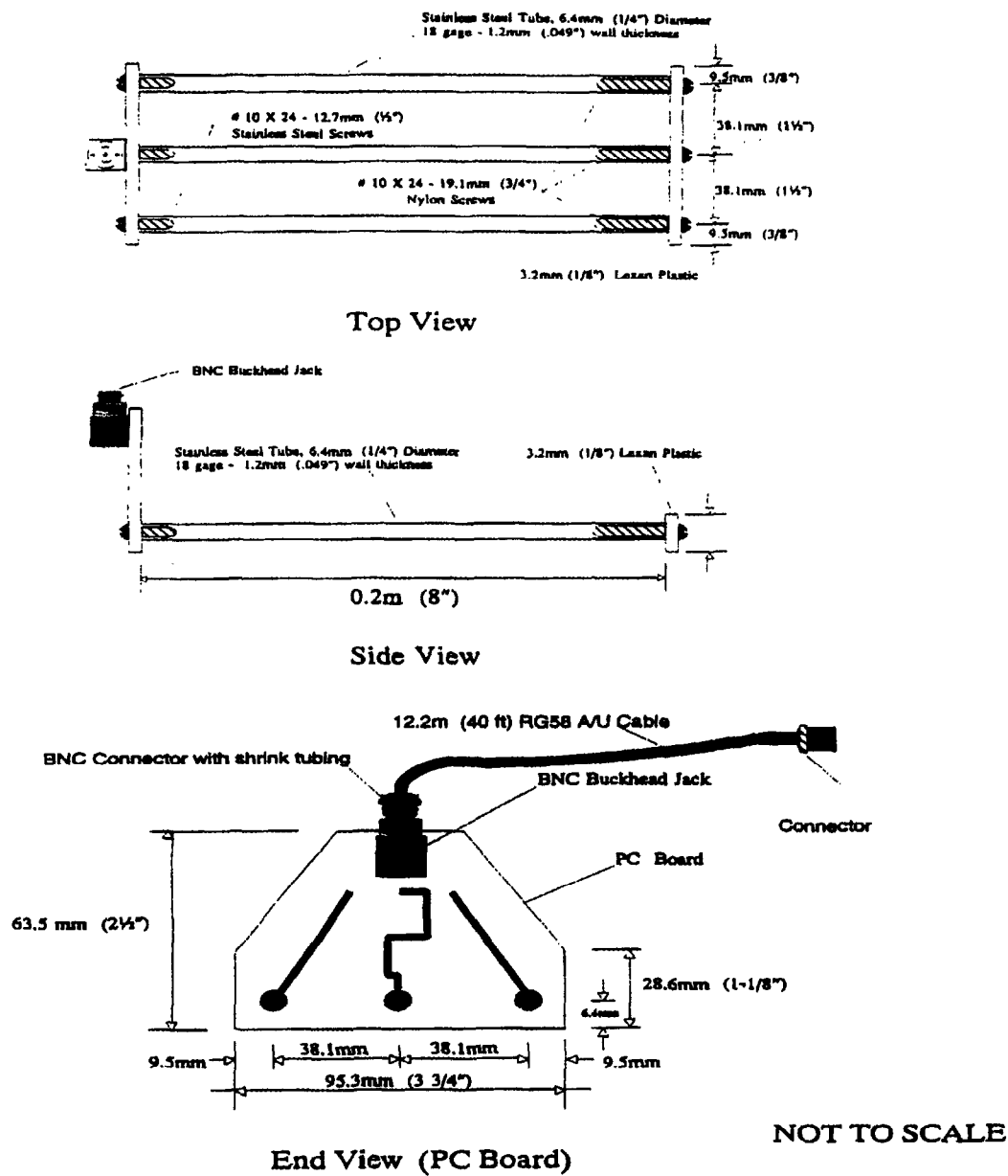
13

Figure 1. TDR Probe Developed by FHWA.

14

A velocity of propagation of 0.99 is used as a constant setting to keep the TDR responses uniform to each other. The vertical scale, with units of decibels, is the only setting adjusted when attempting to maximize the resolution of each waveform in the display. The waveform is normally adjusted to fit the upper and lower vertical limits of the display. This aids in interpreting the apparent length of the TDR trace.

An RS232 (SP232) interface is used in the Tektronix unit to allow the cable reader to transfer the TDR response to a portable computer. In addition to this interface, software developed by Tektronix is used to visualize and/or store the TDR response as an ASCII data file to the computer.

The FHWA TDR three-prong probe (each prong is 0.203 m in length) is connected to the 1502C by a 50-ohm coaxial cable 13.1 m in length. It has been found that as the length of the cable increases (approaches 33 m), the signal becomes weaker, i.e., more difficult to read.

A Toshiba T4600c PC is used for the collection of TDR responses. Each TDR response is saved to a data file containing 251 points. This permanent record allows for additional analysis to be conducted.

Other equipment needed in support of the lab testing includes an oven to dry the soil sample to obtain the gravimetric moisture content, and two scales: one to weigh a small sample of soil to calculate the gravimetric moisture content, and a larger scale capable of weighing up to 18 kg of soil. A mold is made from a 0.254-m-diameter Sonotube. The mold is cut in half and attached to the vibratory table by angle brackets. Since compaction of the soil is necessary, a vibratory table is needed. Lead weights up to 77 kg are used as a surcharge to compact the soil sample.

LABORATORY PROCEDURE

The laboratory study consisted of testing 28 soil samples for their TDR response. An ASCII data file for each soil sample, level of moisture, and level of compaction was recorded.

A Sonotube with a 0.254-m inside diameter and a height of 0.33 m was used as a mold to test each soil sample. To extract the soil sample easily from the mold, the mold was cut in half to act as a split mold. This permitted testing the soil sample to determine whether the mold interfered with the TDR reading of the apparent length. The Sonotube was attached to a vibratory table by brackets, which were fastened to the table. The Sonotube was fastened together with a metal band to maintain a constant volume, permitting a calculation of the volume of soil inside the mold. A 0.019-m-thick x 0.254-m-diameter piece of plywood was placed on the bottom of the mold to reduce the effects of any reflected electromagnetic waveforms.

A soil sample, at a uniform moisture content, was weighed and then added to the mold until approximately 0.10 m of soil filled the bottom of the mold. The TDR probe was then placed horizontally in the mold, with the coaxial cable placed against the side of the mold. The remaining amount of soil was added to the mold until the probe was covered with approximately 0.153 m of soil. A 0.254-m-diameter circular disk fabricated of metal with a half-moon shape was cut in one side to allow the coaxial cable to pass through.

Measurements were taken at each moisture and density level combination. This information included: sample identification number, weight of load applied, vibration amplitude, total weight of the soil sample in the mold, and height of the soil from the top of the mold when the desired weight–time relationship was achieved. The first TDR trace was recorded when all the soil was added to the mold and very little compaction had occurred. A 10.17-kg surcharge was placed on the soil sample and vibrated for 30 s. The weights were removed and a second TDR trace was recorded. A 45.05-kg surcharge was then placed on the soil sample and vibrated for 1 min. The weight was then removed and a third TDR trace was recorded. A 77.20-kg surcharge was placed on the soil sample and vibrated for 1 min. The weight was removed and a fourth TDR trace was recorded. A modified proctor hammer was then dropped a few times on the soil sample. If the soil demonstrated signs of additional compaction, 50 blows were dropped onto the sample and a fifth TDR trace was recorded. If the soil did not show signs of additional compaction, the testing was considered to be complete and two samples were taken to determine the gravimetric moisture. If the soil sample would compact more, an additional 50 blows were dropped on the soil sample. A sixth and final TDR measurement was recorded.

A moisture sample was taken by splitting the mold in half and carefully removing the soil from the TDR probe. Two moisture samples were taken from the soil between the TDR prongs. These samples were dried in an oven at 110° C for 24 h. The gravimetric moisture content was calculated after the dried soil weighed a constant weight. The total soil weight, gravimetric moisture content, specific gravity, and total volume of the mold were used to calculate the porosity, bulk density, and degree of saturation.

CHAPTER IV: PHASE I STUDY

APPARENT LENGTH

Because the dielectric constant (K_a) is proportional to the square of the apparent length (L_a), errors or differences in the measured L_a will significantly influence the computed (measured) K_a value of the soil mixture. The purpose of the initial phase of this study was to identify the best method for determining the apparent length of the TDR probe when calculating the dielectric constant.

From the literature review, the five known methods for calculating the dielectric constant from the TDR trace are:

- Method of Tangents ([1,5,6]).
- Method of Peaks ([1,15]).
- Method of Diverging Lines ([1]).
- Alternate Method of Tangents ([1]).
- Campbell Scientific Method ([25], unpublished data).

Each method uses a slightly different location to measure the initial and final inflection points of the trace signal. Figures 2 through 6 illustrate a typical TDR trace and the relative interpretation methodology of the L_a value for each of the five methods.

The Method of Tangents approach, shown in figure 2, determines the initial inflection point (point A) by locating the intersection of the horizontal and negatively sloped tangents at the trace's local maximum value. The final inflection point (point B) is located at the intersection of the horizontal and positively sloped tangents to the trace's local minimum value.
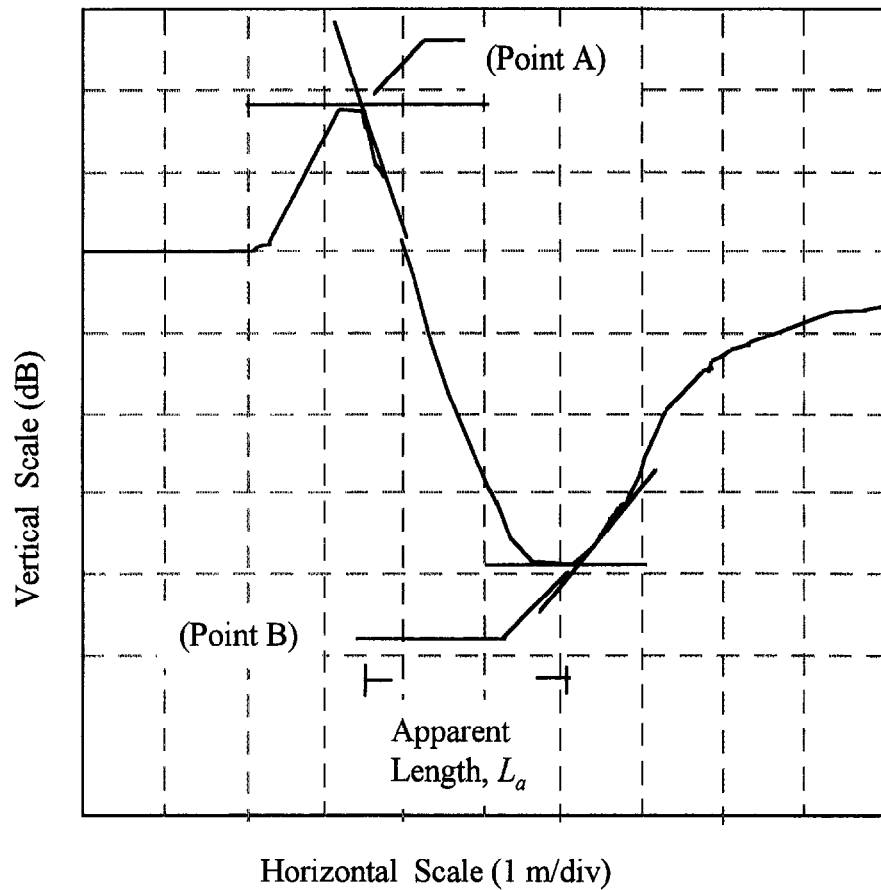
Figure 2. Method of Tangents.

Figure 3 illustrates the Method of Peaks procedure. The initial inflection point (point A) is determined by locating the intersection of the tangents drawn on either side of the local maximum. The final inflection point (point B) is located at the intersection of the tangents drawn on both sides of the local minimum.
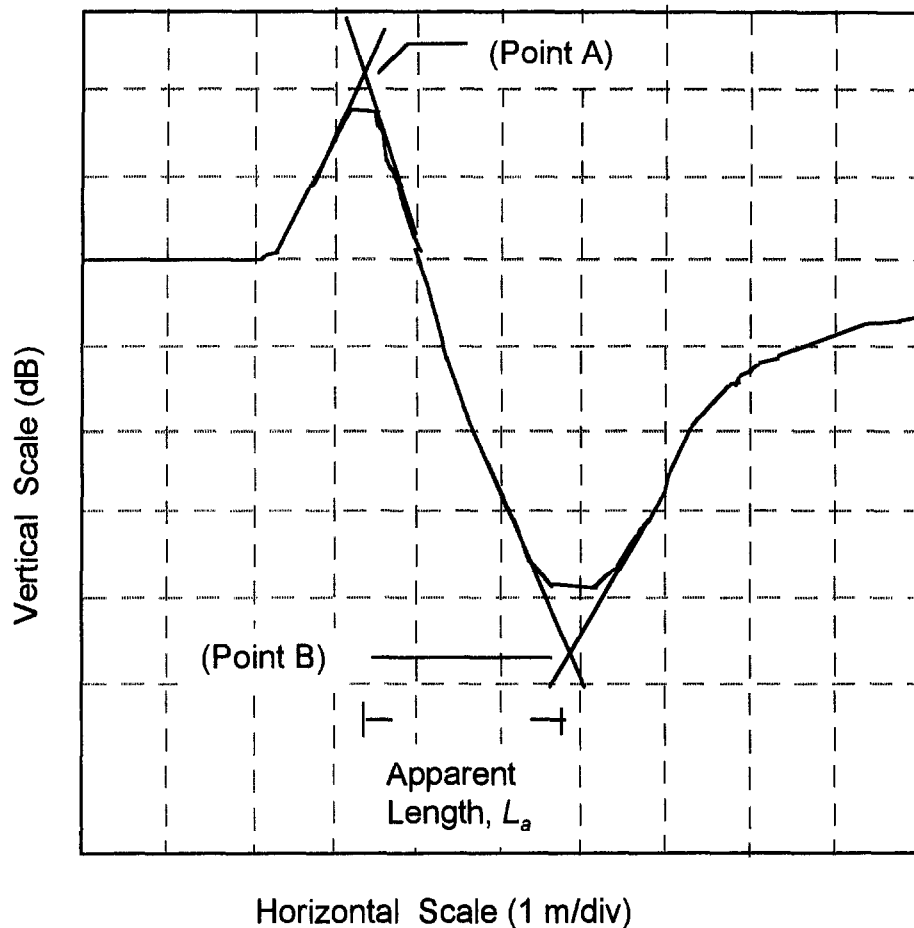
Figure 3. Method of Peaks.

The Method of Diverging Lines, shown in figure 4, determines the initial inflection point (point A) to be where the trace diverges from the local maximum's positively sloped tangent. The final inflection point (point B) is located where the trace diverges from the local minimum's negatively sloped tangent.
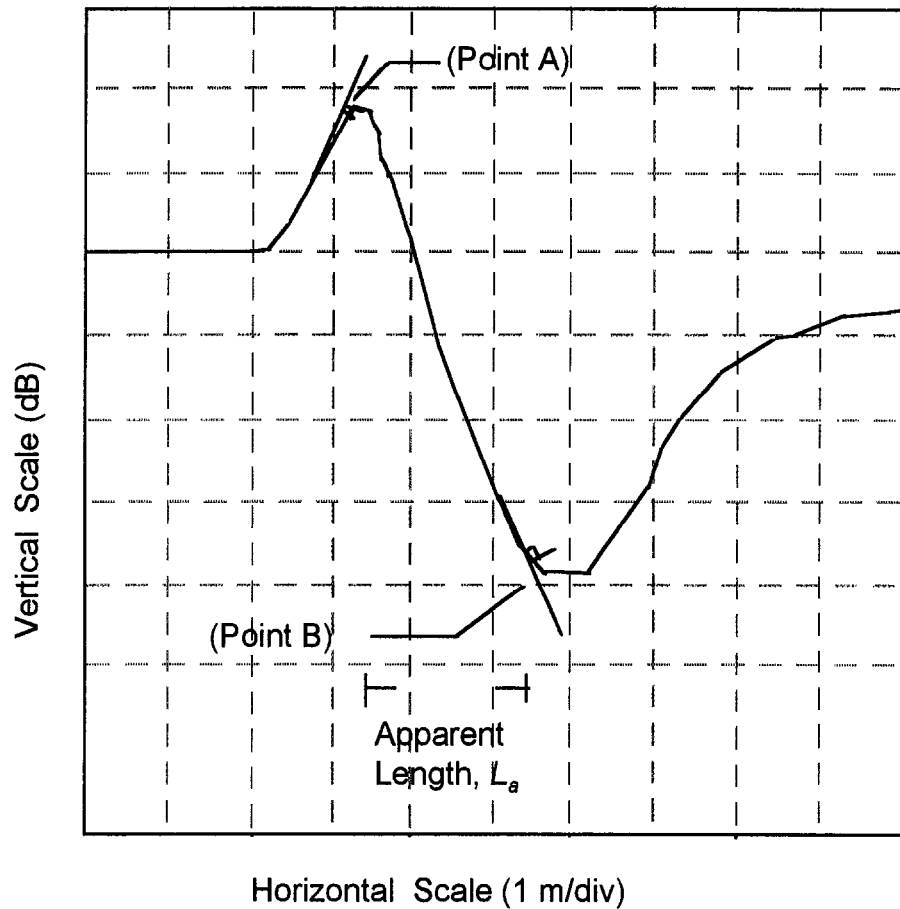
Figure 4. Method of Diverging Lines.

In figure 5, the Alternate Method of Tangents approach is shown. The initial inflection point (point A) is determined by locating the intersection of the horizontal and positively sloped tangents at the trace's local maximum value. The final inflection point (point B) is located at the intersection of the horizontal and negatively sloped tangents to the trace's local minimum value.
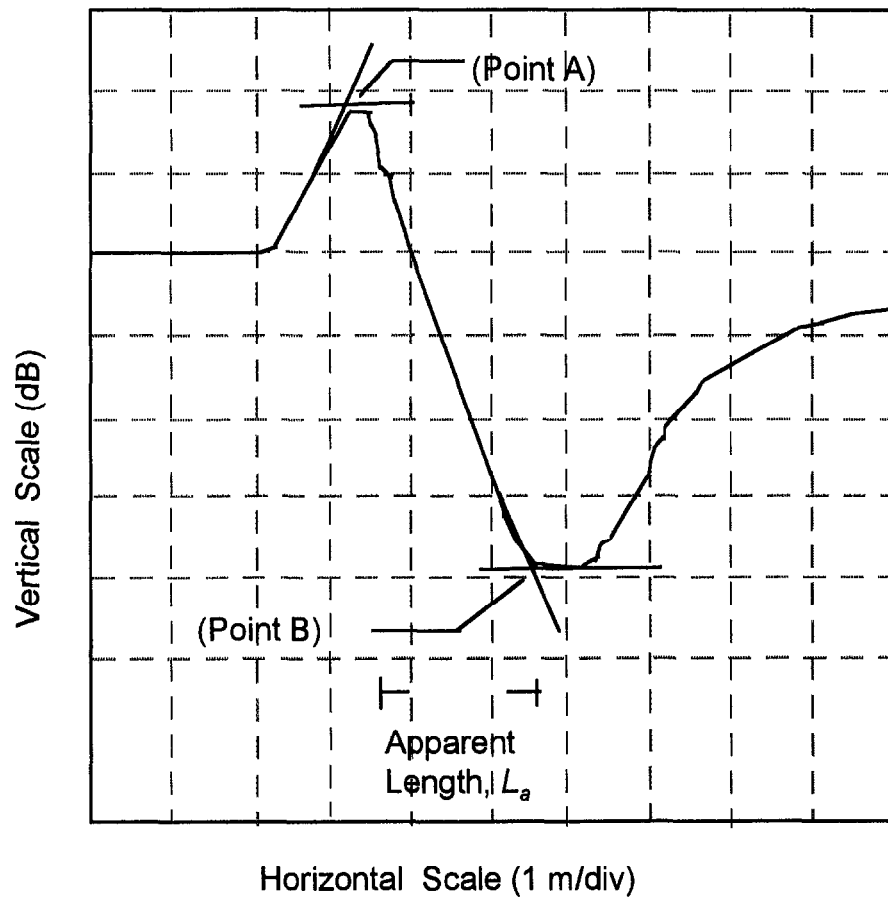

Figure 5. Alternate Method of Tangents.

Finally, the Campbell Scientific Method is shown in figure 6. The initial inflection point (point A) is found where the coaxial cable connects to the TDR probe. This inflection point is located at the intersection of the horizontally sloped line prior to the increase in voltage and the positively sloped tangent to the increase in voltage. The final inflection point (point B) is located at the intersection of the tangents drawn on both sides of the local minimum. Laboratory testing is required to determine the travel time of the material from the coaxial cable to the beginning of the actual probe. This travel time is subtracted from the total travel time to give a better approximation of the apparent length.

Figure 6. Campbell Scientific Method.

STUDY APPROACH
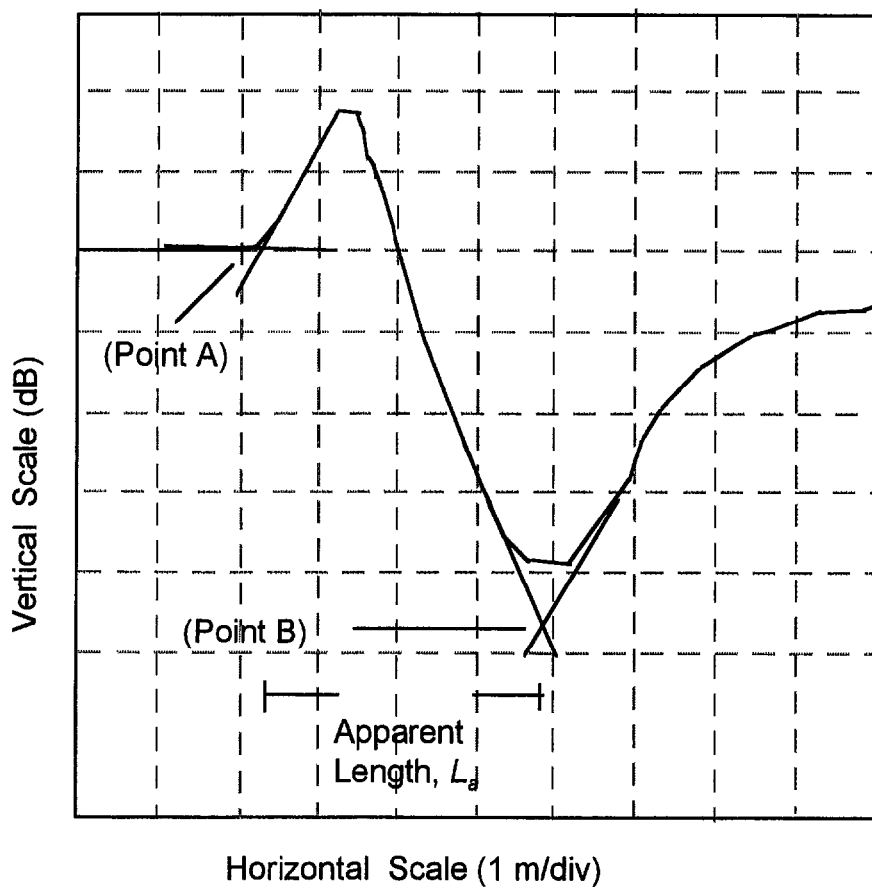
Soil samples from 28 LTPP General Pavement Study sites in the United States and Canada were obtained from the LTPP-SMP. Table 2 summarizes the American Association of State and Highway Officials (AASHTO) classification of the LTPP section materials used in the study.

Each of the five methods was evaluated using each soil sample. The soil samples were compacted at three levels of moisture and five levels of compaction. The initial laboratory study resulted in a total of 361 soil-mixture TDR signal traces from the FHWA TDR probe design. These traces were used to evaluate the L_a (K_a) determined by each method.

For each soil sample test, mass (wet) densities and gravimetric moisture contents (taken between the TDR prongs) were completed. Knowledge of the specific gravity, G_s, from the LTPP database permitted the computation of all pertinent gravimetric and volumetric properties of each compacted soil sample.

To select the most accurate L_a computational methodology, the scatter (error) found between specific regression relationships of L_a (K_a) to the volumetric moisture content (V_w) was statistically evaluated for each of the five methodologies. Goodness-of-fit statistics were used to evaluate each method [e.g., explained variance (R^2), standard error ratio (Se/Sy), and the relative error ($\acute{e}/\acute{y}$)]. For the purpose of fitting each line (L_a methodology), a regression analysis was conducted using a model that gave the best fit, as well as rational coefficients.

Table 2. Summary of Soil Types by AASHTO Classification.

Major Soil Type	AASHTO	LTPP Sample
Coarse grained	A-1-b	271028
	A-1-b	271018
	A-2-4	831801
	A-2-4	404165
	A-2-4	161010
	A-2-4	484142
	A-2-4	231026
	A-2-4	364018
	A-2-4	493001
	A-2-4	561007
	A-2-4	491001
	A-3	893015
	A-3	331001
	A-3	251002
	A-3	276251
	A-3	351112
	A-3	483739
	A-3	481122
Fine grained	A-4	906405
	A-4	481077
	A-4	871622
	A-4	091083
	A-6	081053
	A-6	460804
	A-7-5	833802
	A-7-5	501002
	A-7-6	469187
	A-7-6	481068

RESULTS ANALYSIS

Apparent Length

An initial evaluation was conducted using the apparent length L_a of each TDR response from the five known methods. A correlation matrix determined that all five methods were highly intercorrelated with each other. This would be expected since all five methods used the same TDR response with slightly different initial and final inflection points. Plots were made to observe the relationship of the apparent length of each method compared to that of the Method of Tangents.

The following results are easily identified from the plots. The first observation is that the Method of Peaks (figure 7a) and the Campbell Scientific Method (figure 7b) have identical patterns relative to the Method of Tangents. The Campbell Scientific Method is slightly higher than the line of equality, since the correction factor due to the printed circuit board was not subtracted from the apparent length. From both figures, it can be observed that approximately 20 data points significantly deviate from the line of equality. These points generally represent the deviations in the procedure used by the Method of Tangents to determine the final inflection point. Overall, both the Method of Peaks and the Campbell Scientific Method have reasonably similar values for the apparent length.

Figure 7a. Apparent Length Comparison of Method of Tangents to Method of Peaks.
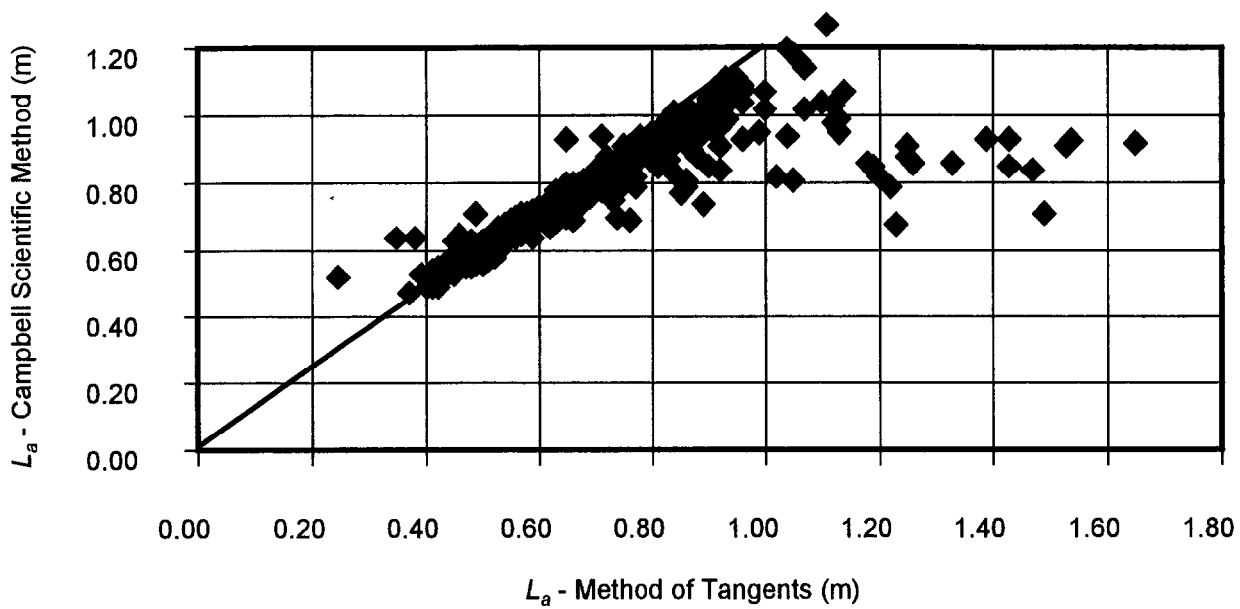
Figure 7b. Apparent Length Comparison of Method of Tangents to Campbell Scientific Method.

The Method of Diverging Lines (figure 7c) and the Alternate Method of Tangents (figure 7d) have a lower apparent length than that of the Method of Tangents. The amount of scatter in figures 7c and 7d is greater than the amount of scatter shown in figures 7a and 7b. This scatter is a result of the means by which these two methods interpret the final inflection point.
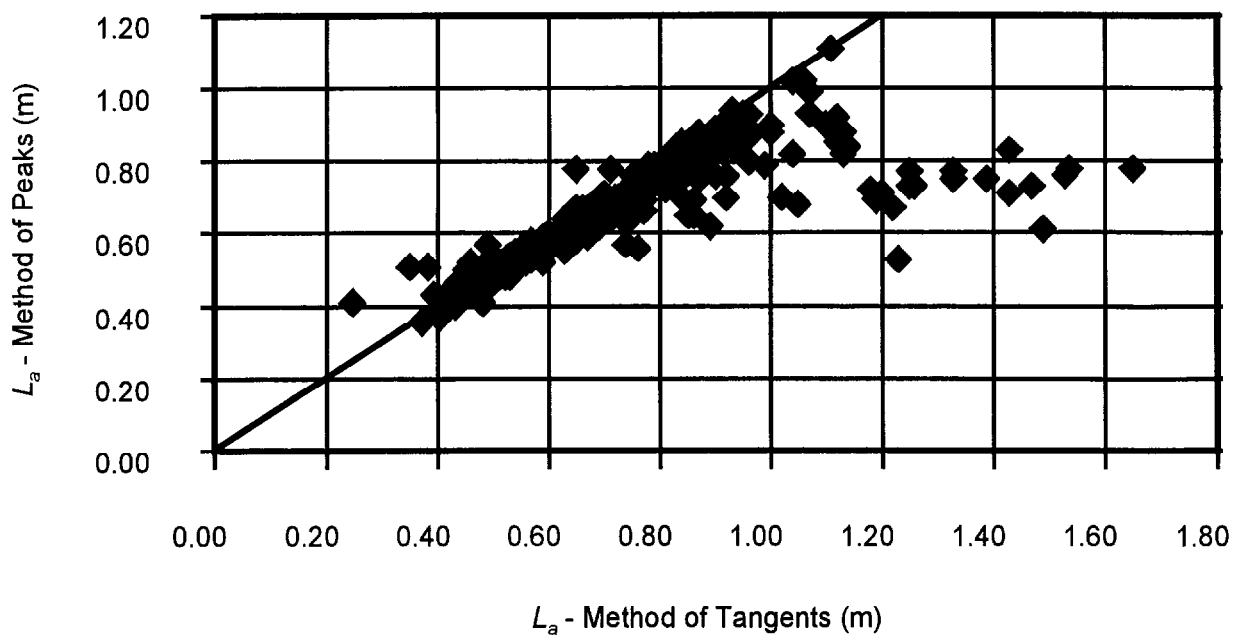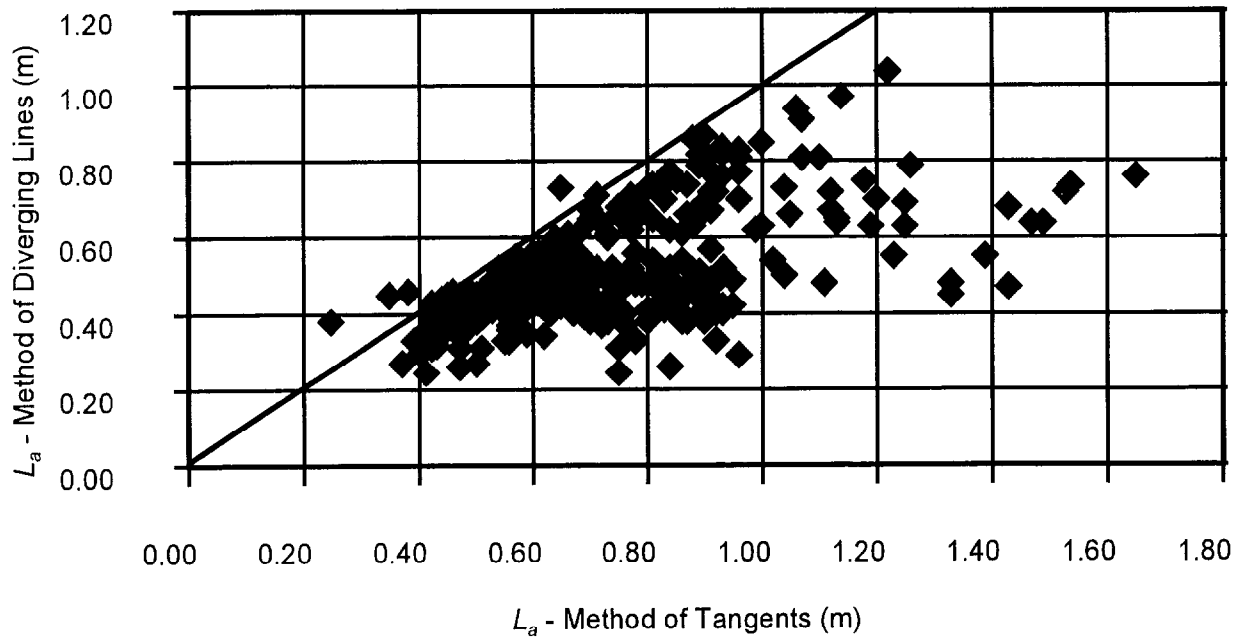

Figure 7c. Apparent Length Comparison of Method of Tangents to
Method of Diverging Lines.
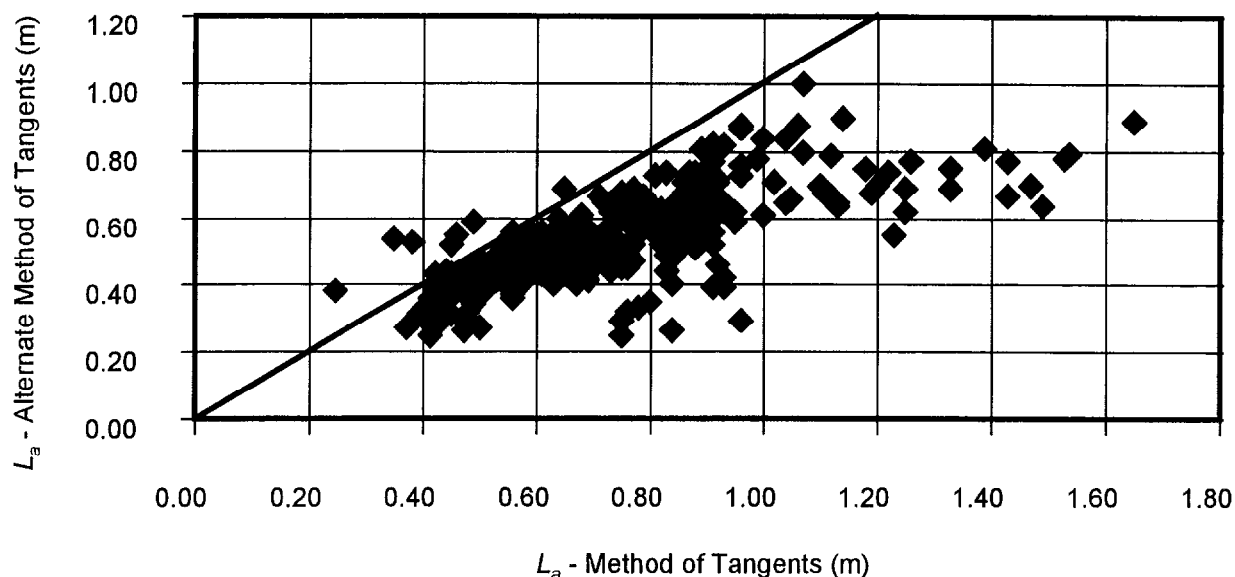
Figure 7d. Apparent Length Comparison of Method of Tangents to
Alternate Method of Tangents.

Statistical Analysis

Statistical models of the volumetric moisture and the dielectric constant (in reality, the apparent length) computed from equation 1 were developed for each method to assess quantitatively the "best" method for determining the L_a value. An examination of the statistical goodness-of-fit parameters for each method was then used to decide which approach provided the "best" methodology.

Most empirical equations for predicting the volumetric moisture content use a third-order polynomial (refer to equations 2 and 3). For the range of volumetric moisture contents used in this study, irrational coefficients for a polynomial model occur in the Method of Tangents, Method of Diverging Lines, and Campbell Scientific Method. In these three cases, the volumetric moisture content decreases as the dielectric moisture content increases in the higher moisture levels. This, of course, is irrational from a theoretical viewpoint.

A power model with a phase shift was used for all models except the Method of Tangents. Due to its larger range of dielectric values, the Method of Tangents was best fitted with a composite model using a power–linear equation with a breakpoint at a

dielectric constant at 35. Although a polynomial could be used for the Method of Peaks and the Alternate Method of Tangents, the explained variance decreased only approximately 1 percent when fitted with a power model.

When the Method of Tangents was used to determine point A and point B, the dielectric constant was calculated for each of the initial 361 laboratory points and plotted in figure 8a.
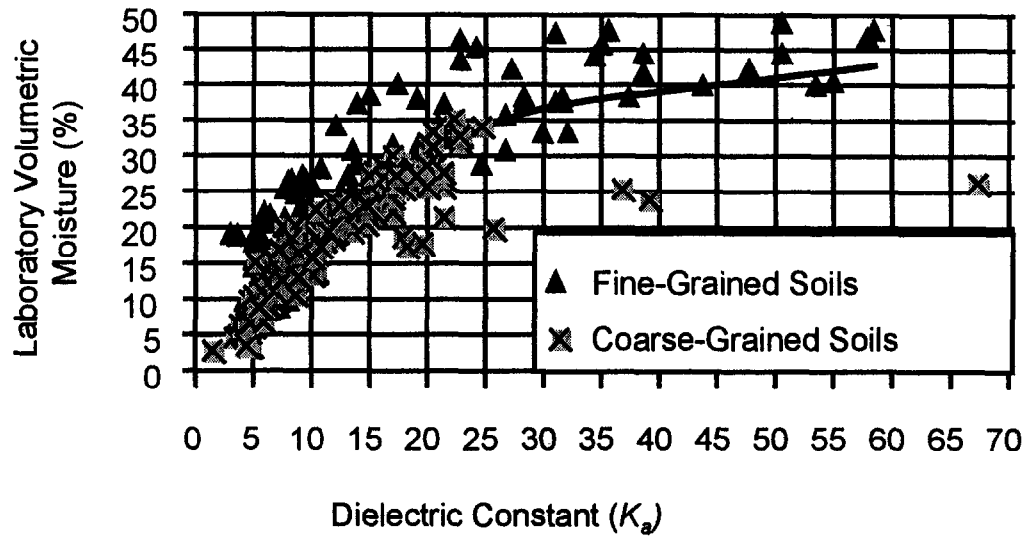
Figure 8a. Method of Tangents Regression Analysis.

A composite model using a power–linear form was chosen for this method. Equation 4 is the composite model used to predict the volumetric moisture content.

$$V_w = (1.8612\,e^{(-0.0263K_a)}\,K_a^{1.1081})\quad if\ (K_a \leq 35)$$

$$V_w = [38.046 + 0.2022(K_a - 35)]\quad if\ (K_a > 35)$$

(4)

This model has an explained variance of 81.0 percent with a Se/Sy of 0.4371. The relative error is 0.0015. There are some areas of local bias, especially where the dielectric

31

constant is less than 7. This method has the highest explained variance and lowest standard error compared to all other methods analyzed.

Figure 8b shows the frequency distribution of the residuals. The Method of Tangents has the best normal distribution of the residuals compared to all other methods. The distribution is also more narrow than the distributions of the other methods.
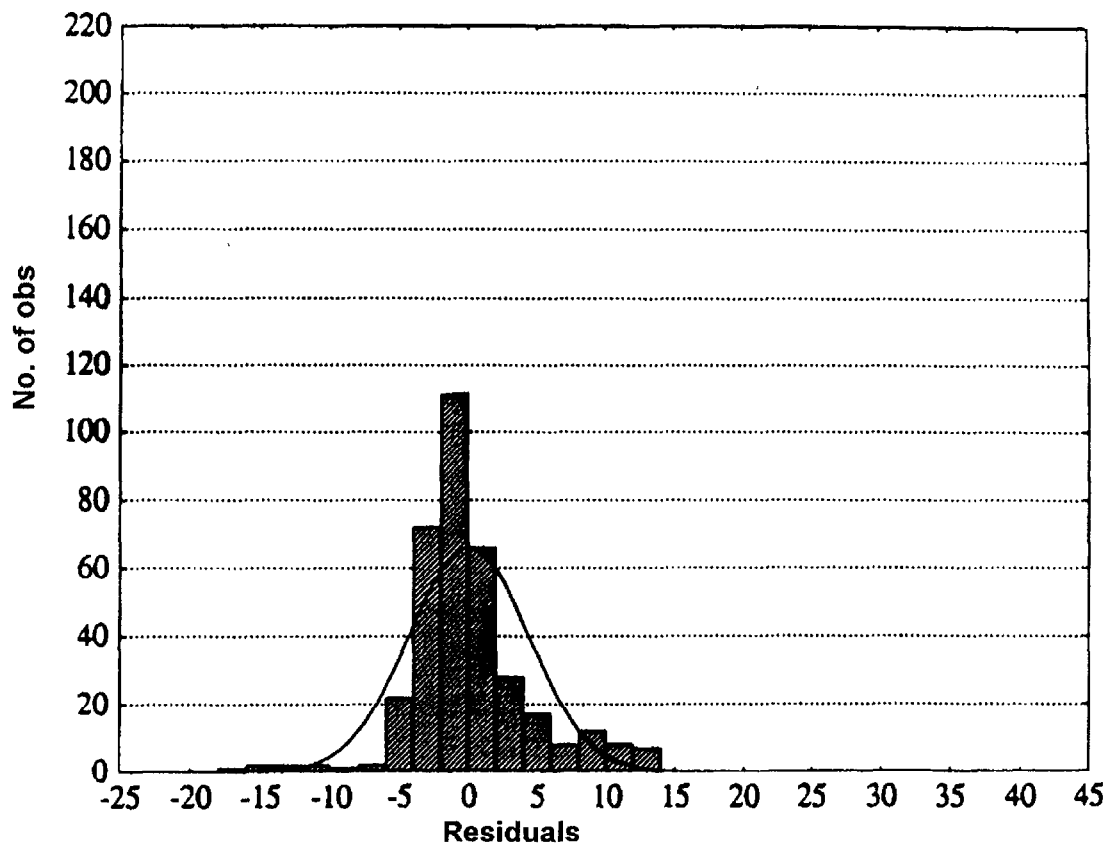
Figure 8b. Method of Tangents Frequency Distribution of Residuals.

When the Method of Peaks was used to determine point A and point B, the dielectric constant was calculated and plotted against the volumetric moisture content, as shown in figure 9a.
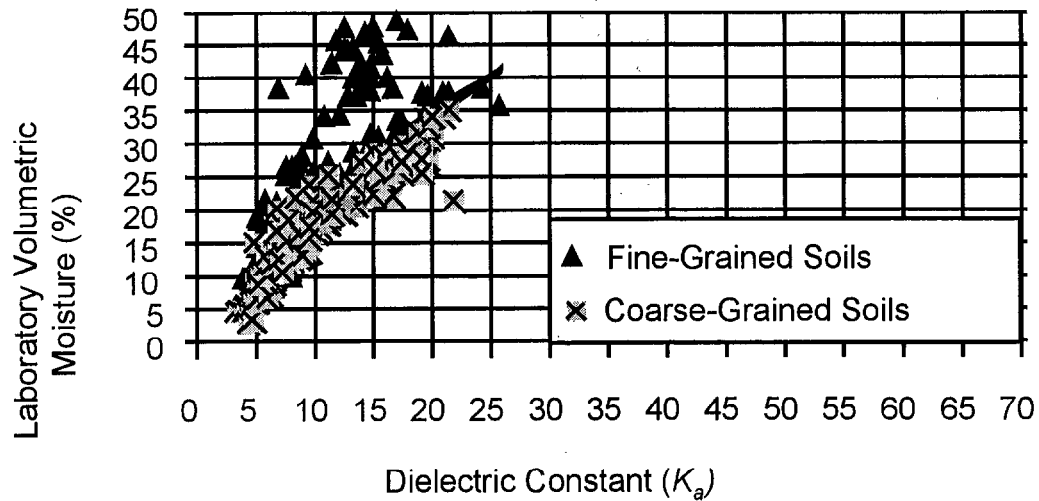
Figure 9a. Method of Peaks Regression Analysis.

A power model was chosen to best fit this method and is shown in equation 5.

$$V_w = 7.1086(K_a - 3.191)^{0.5624} \qquad (5)$$

A third-order polynomial fits this method with an explained variance of 67.54 percent. The power model has an explained variance of 66.35 percent—1.2 percent lower than the polynomial. The Se/Sy is 0.5809 with a relative error of 0.00263. There are also some areas of local bias, especially at the lower dielectric constant values. Figure 9b shows the frequency distribution of the residuals.
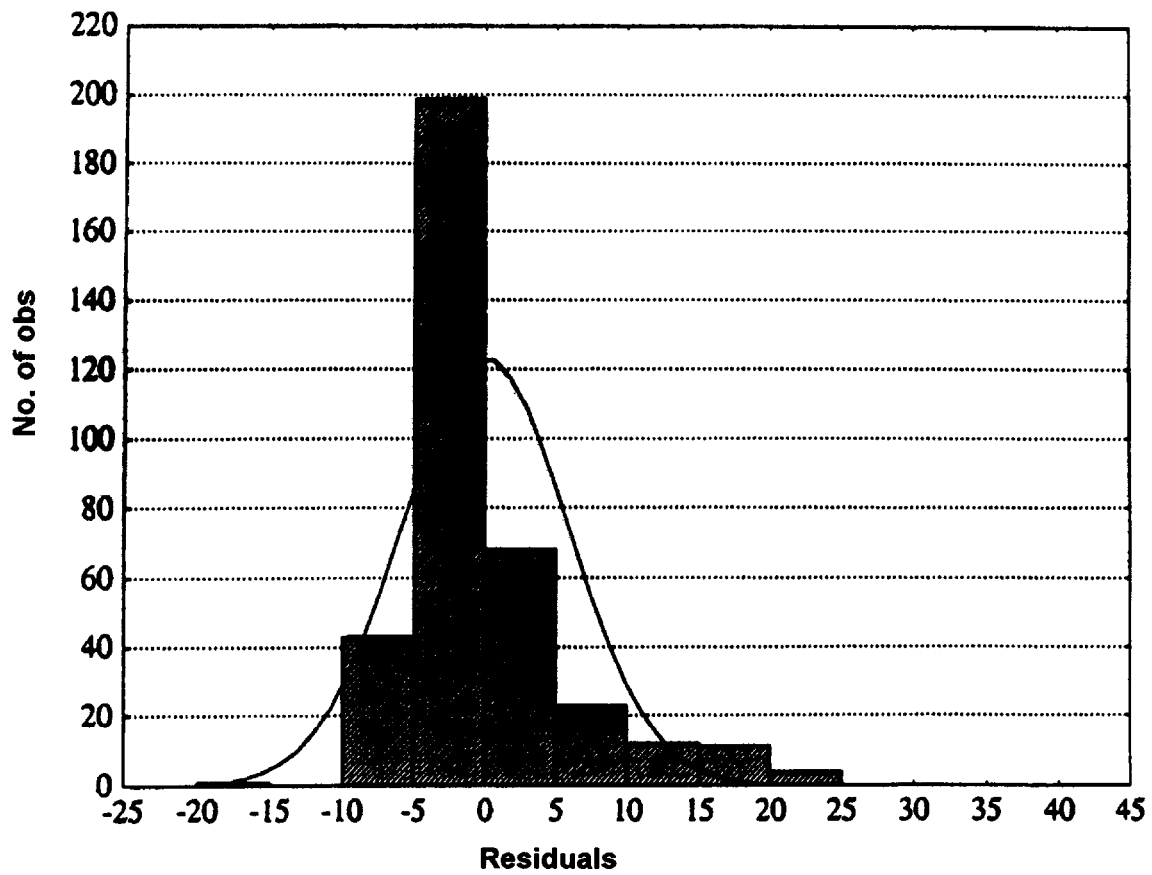
Figure 9b. Method of Peaks Frequency Distribution of Residuals.

As shown in figure 10a, the Method of Diverging Lines displays a large percentage of data points clustering around a dielectric value of 5 with increasing volumetric moisture content. This theoretically violates the concept of proportionality of the dielectric constant to volumetric moisture. In this methodology, a polynomial is irrational, since an increase in dielectric values would lead to decreasing volumetric moisture content.
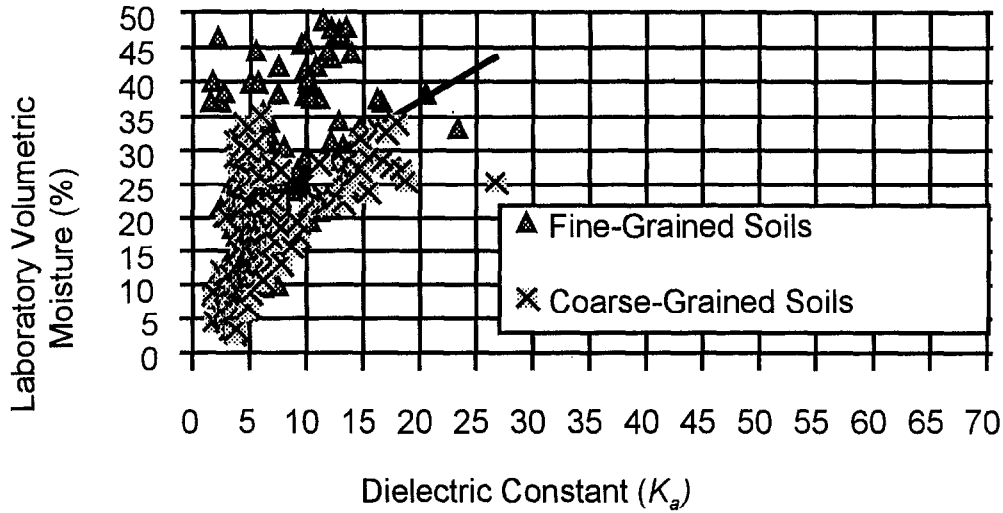
Figure 10a. Method of Diverging Lines Regression Analysis.

The best-fit model for this method of determining L_a is shown in equation 6.

$$V_w = 7.4546(K_a + 0.2519)^{0.5360}$$

(6)

This model has an explained variance of 30.73 percent, by far the lowest of all five methods. In this method, it is very difficult to analyze each trace, since identifying initial and final inflection points is highly subjective. The Se/Sy is 0.8334 with a relative error equal to 0.0006. The residuals are the lowest of the five methods, but this is due to the large amount of symmetrical scatter on both sides of the predicted volumetric moisture line. Figure 10b shows the frequency distribution of the residuals.
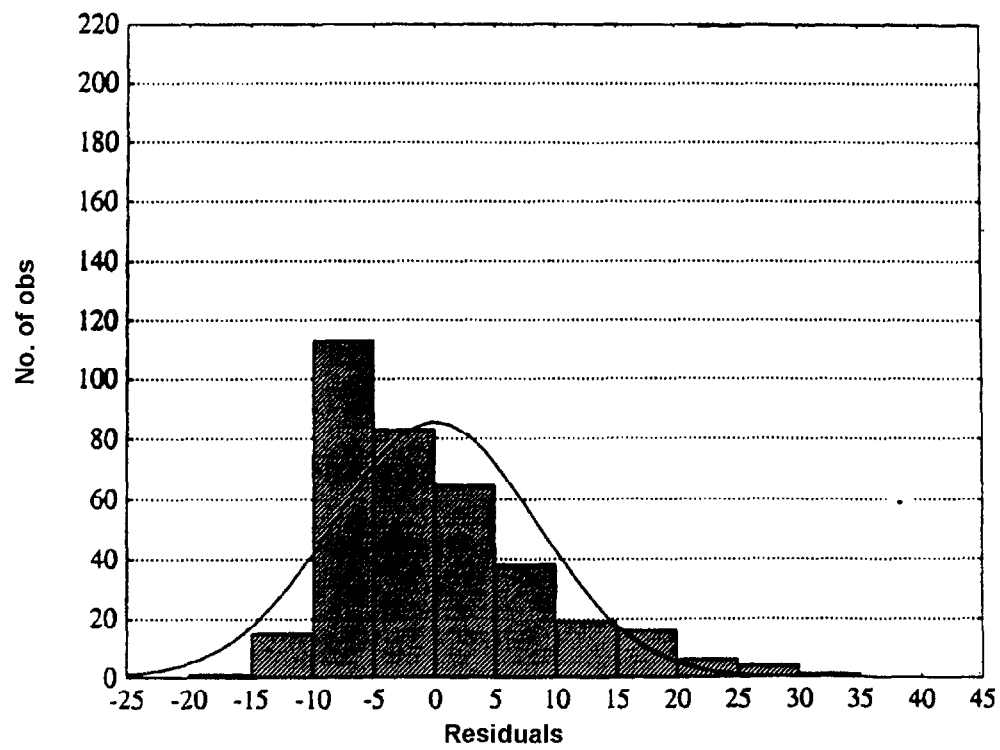
Figure 10b. Method of Diverging Lines Frequency Distribution of Residuals.

When the Alternate Method of Tangents was used to determine point A and point B, the dielectric constant was calculated and plotted (as shown in figure 11a) for each of the 361 laboratory points. A second-order polynomial model was then used, with an explained variance of 52.7 percent.
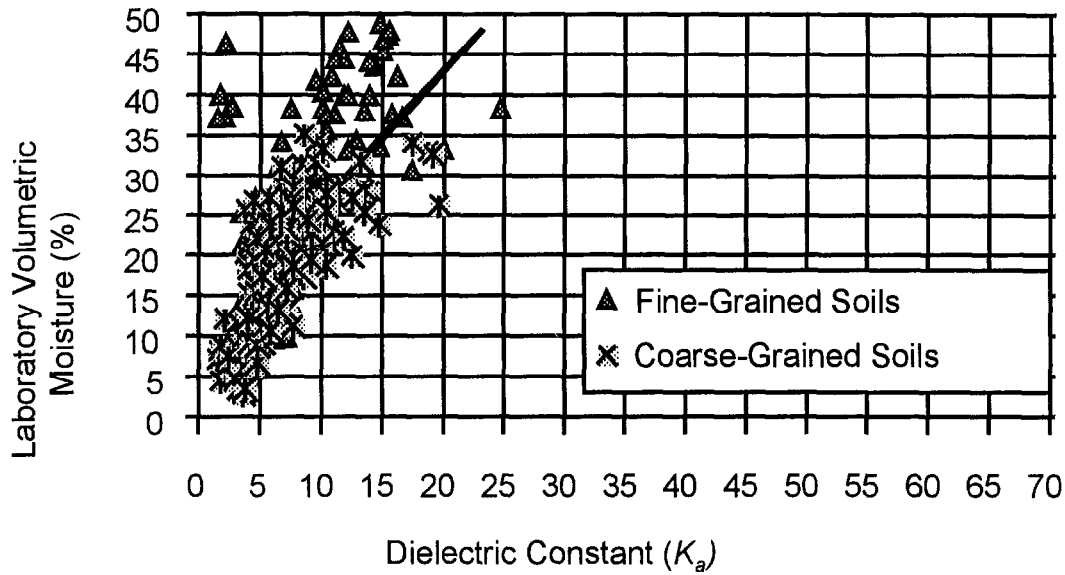
Figure 11a. Alternate Method of Tangents Regression Analysis.

Equation 7, however, uses the form of a power model to estimate the volumetric moisture content.

$$V_w = 4.6217(K_a + 0.3528)^{0.7510}$$ (7)

This model has an explained variance of 51.27 percent. This is 1.4 percent lower than the polynomial model. The Se/Sy of the power model is 0.6990 with a relative error of 0.00063. Figure 11b plots the frequency distribution of the residuals using the power model for the Alternate Method of Tangents.
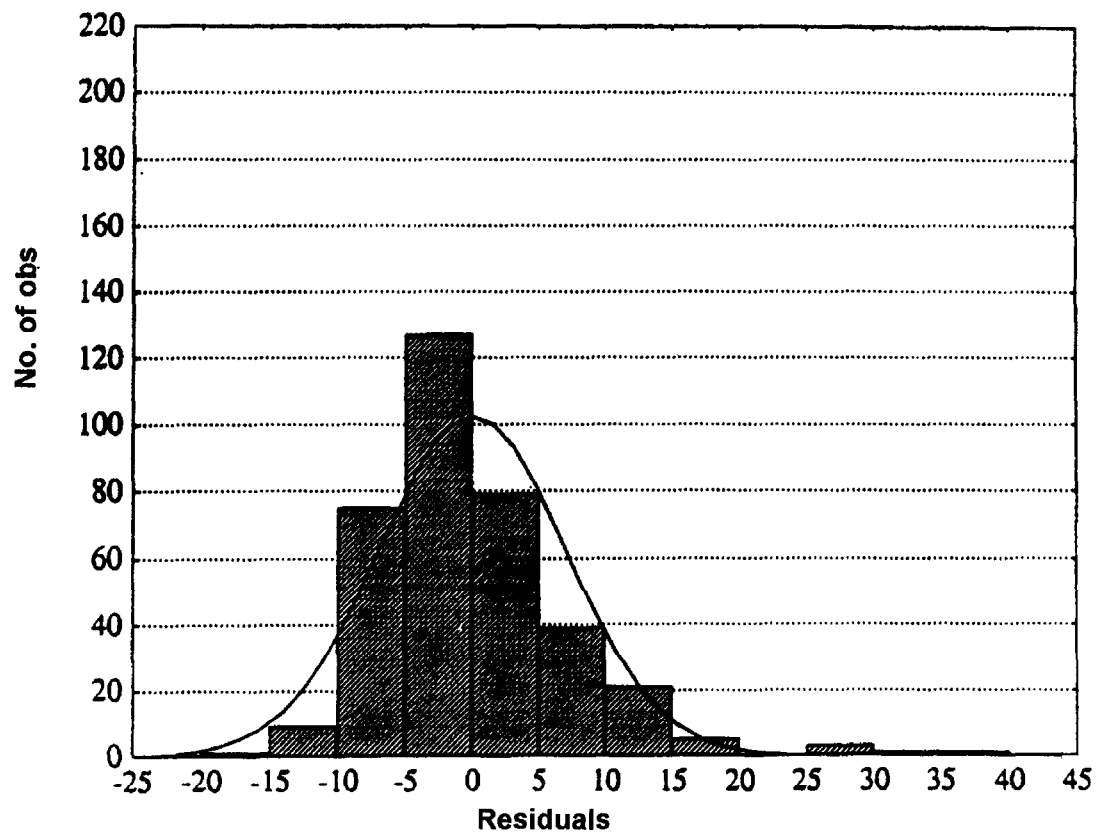
Figure 11b. Alternate Method of Tangents Frequency Distribution of Residuals.

When the Campbell Scientific Method was used to determine the initial and final inflection points, the dielectric constant was calculated and plotted with volumetric moisture content as shown in figure 12a. A polynomial could not be used since the increase in dielectric constant did not yield an increase in volumetric moisture content for the higher moisture levels.
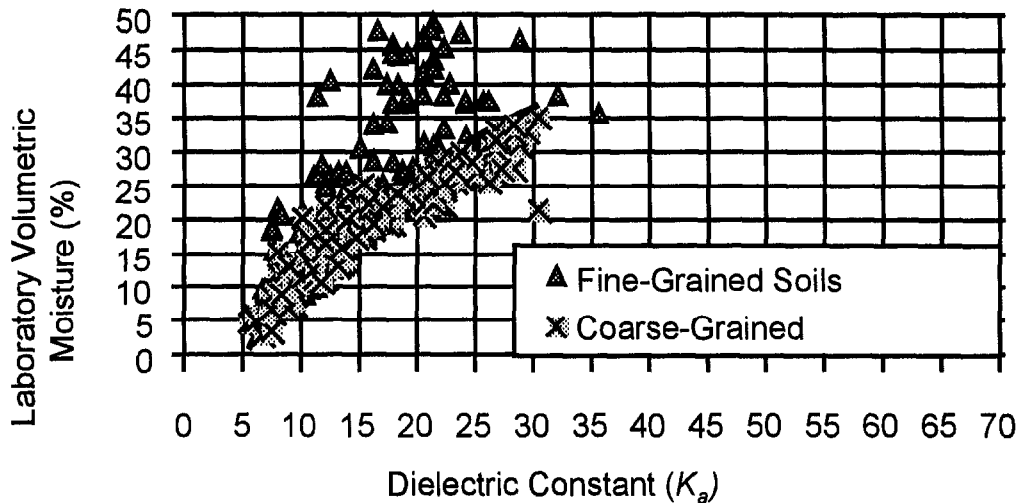
Figure 12a. Campbell Scientific Method Regression Analysis.

The best power model used to estimate the volumetric moisture is shown in equation 8.

$$V_w = 6.043(K_a - 5.4749)^{0.5634} \tag{8}$$

This model has an explained variance of 64.55 percent and a Se/Sy of 0.5961. The relative error equals 0.0020, with areas of local bias present. Note must be taken that a correction factor must be used to account for the travel time of the printed circuit board. This correction factor in L_a is constant for all data points. Figure 12b plots the frequency distribution of the residuals using the power model.
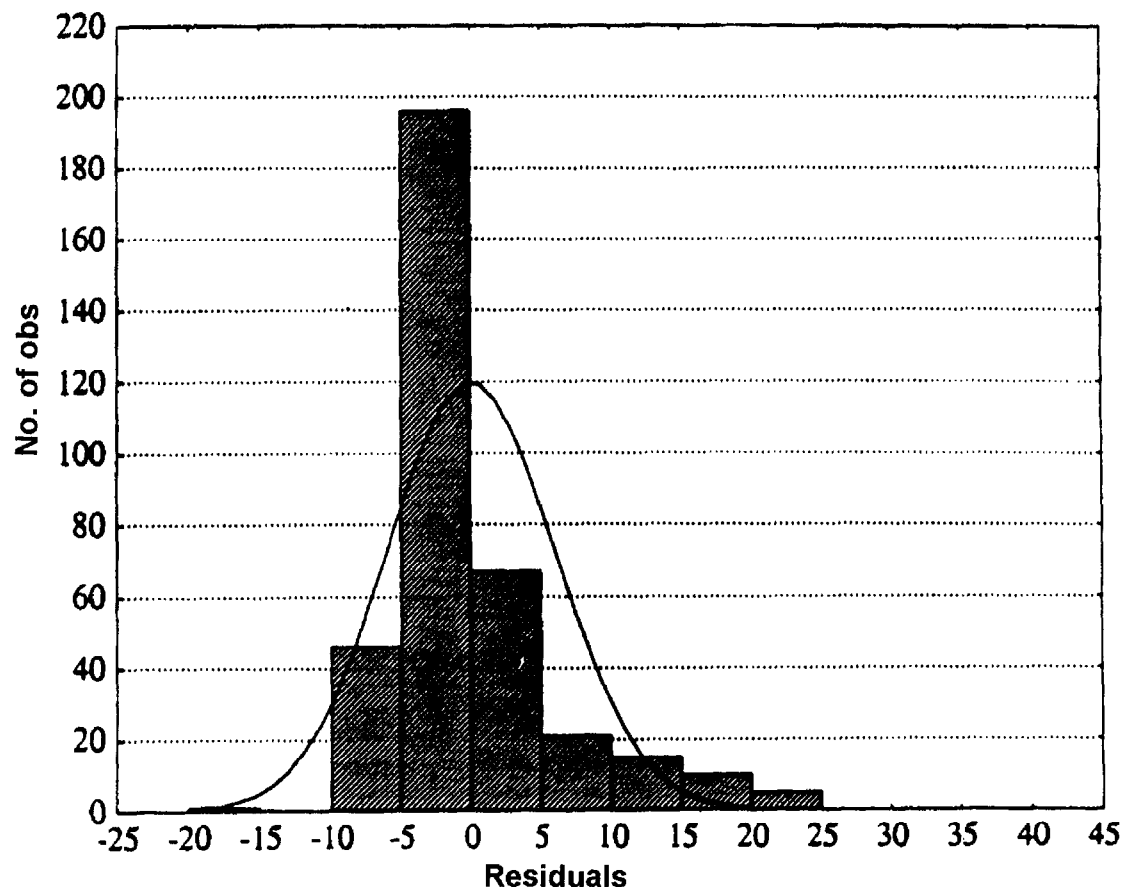
Figure 12b. Campbell Scientific Method Frequency Distribution of Residuals.

SUMMARY

It can be concluded from the analysis and results presented that there are significant differences between the various methods used to establish the apparent length L_a and hence the dielectric constant. These difference are due to the locations used to define the initial and final inflection points of the TDR response signal for each method. While all of the methods possess high intercorrelations, differences in the measured L_a do significantly influence the predictive models and their associated accuracy.

Table 3 is a master summary of the goodness-of-fit statistics for all five methods investigated. As measured by R^2, Se, and the Se/Sy ratio, it can be observed that the most accurate method is the Method of Tangents, while the least accurate methods are the Alternate Method of Tangents and the Method of Diverging Lines. The Method of Peaks and Campbell Scientific Method yield very similar goodness-of-fit statistics, due to the fact that for all practical matters, they measure identical L_a values. Both of these methods yield goodness-of-fit parameters that are slightly inferior to those determined for the Method of Tangents.

Table 3. Results of Statistical Analyses.

Model	Model	R^2	Se	Se/Sy	e	e/y
Method of Tangents**	Poly.	81.2	4.59	0.45	0.3479	0.01727
	Comp.	81.0	4.44	0.43	0.0303	0.00150
Method of Peaks	Poly.	67.5	5.80	0.57	-0.0143	-0.00071
	Power	66.4	5.90	0.58	0.0530	0.00263
Method of Diverging Lines	Poly.	32.8	8.34	0.82	0.0007	0.00004
	Power	30.7	8.47	0.83	0.0122	0.00060
Alternate Method of Tangents	Poly.	52.7	7.00	0.69	-0.0028	-0.00014
	Power	51.3	7.10	0.70	0.0126	0.00063
Campbell Scientific Method	Poly.	66.1	5.92	0.58	0.0112	0.00056
	Power	64.6	6.06	0.60	0.0412	0.00204

** This method was fitted with a composite model consisting of a power–linear form with a breakpoint at $K_a = 35$.

41

CHAPTER V: PHASE II STUDY

MODEL DEVELOPMENT

Two different approaches are used to relate soil volumetric moisture content to the TDR response. The first approach is empirical. It selects functional relationships based on their mathematical flexibility to fit the experimental data points.

The second approach derives a mechanistic or fundamental equation from the dielectric mixing models. The fundamental equation relates the composite dielectric number of a multiphase mixture to the dielectric numbers and volume fractions of its constituents. In this approach, the soil is considered to be a three-phase mixture of soil, water, and air. Using the volumetric properties of the soil, such as dry density and specific gravity, in addition to the dielectric values of water and air, we derived a mixing model. The following derivation separates the soil's elements to assume a mixing/composite model of the form:

$$K_a^\alpha = \frac{\sum V_i \in_i^\alpha}{\sum V_i} \tag{9}$$

where:

V_i = volume of ith material phase.

e_i = dielectric constant of ith material.

a = assumed power coefficient.

Letting $V_t = \sum V_i$,

$$K_a^\alpha = \frac{V_s}{V_T}\varepsilon_s^\alpha + \frac{V_a}{V_T}\varepsilon_a^\alpha + \frac{V_w}{V_T}\varepsilon_w^\alpha \tag{10}$$

For a soil mixture with: "s" = solid, "a" = air, and "w" = water,

$$\frac{V_s}{V_T} = \frac{W_s}{G_s \gamma_w V_T} = \frac{\gamma_d}{G_s \gamma_w} = V_s(\%) \tag{11}$$

Since $e_a = 1$ (dielectric constant of air)

$$K_a^\alpha = \frac{\gamma_d}{G_s \gamma_w} \varepsilon_s^\alpha + V_a(\%) - V_a(\%) + V_w(\%) \varepsilon_w^\alpha \qquad (12)$$

where:

$V_a(\%) = V_a/V_T$ (vol. air content)

$V_w(\%) = V_w/V_T$ (vol. water content)

Since $V_a(\%) = 1 - [V_s(\%) + V_w(\%)]$ $\qquad (13)$

$$K_a^\alpha = \frac{\gamma_d}{G_s \gamma_w} \varepsilon_s^\alpha + 1 - V_s(\%) - V_w(\%) + V_w(\%) \varepsilon_w^\alpha \qquad (14)$$

or

$$K_a^\alpha = \frac{\gamma_d}{G_s \gamma_w} \varepsilon_s^\alpha - \frac{\gamma_d}{G_s \gamma_w} + V_w(\%)[\varepsilon_W^\alpha - 1] + 1 \qquad (15)$$

or

$$K_a^\alpha = \frac{\gamma_d}{G_s \gamma_w}(\varepsilon_s^\alpha - 1) + V_w(\%)[\varepsilon_w^\alpha - 1] + 1 \qquad (16)$$

as

$$K_a = (\frac{L_a}{L_p V_p})^2 \qquad (17)$$

where:

L_a = apparent length.

L_p = actual probe length (0.203m).

V_p = velocity of propagation (0.99).

Note that $L_p * V_p = 0.203(0.99) = 0.201 = 1/5$

or $K_a = (5L_a)^2$.

Therefore:

$$K_a^\alpha = (5L_a)^{2\alpha} = \frac{\gamma_d}{G_s\gamma_w}(\varepsilon_s^\alpha - 1) + V_w(\%)[\varepsilon_w^\alpha - 1] + 1 \qquad (18)$$

$$(5L_a)^{2\alpha} - 1 = (\varepsilon_s^\alpha - 1)\frac{\gamma_d}{G_s\gamma_w} + (\varepsilon_w^\alpha - 1)V_w(\%) \qquad (19)$$

This model form can be viewed as:

$$y = (5L_a)^{2\alpha} - 1 = \beta_0\frac{\gamma_d}{G_s\gamma_w} + \beta_1 V_w(\%) \qquad (20)$$

or

$$y = \beta_0 x_1 + \beta_1 x_2 \qquad (21)$$

where:

$b_0 = e_s{}^a - 1$ (22)

$b_1 = e_w{}^a - 1$ (23)

$x_1 = V_s(\%) = \gamma_d/G_s\gamma_w$ (24)

$x_2 = V_w(\%)$ (25)

For the assumption that $a = \frac{1}{2}$, the model reduces to:

$$y = (5L_a - 1) = \beta_0\frac{\gamma_d}{G_s\gamma_w} + \beta_1 V_w(\%) \qquad (26)$$

From equation (26), it is obvious that the values of b_0 and b_1 can be found by linear regression techniques, where:

$b_0 = [SQRT(e_s) - 1]$ (27)

$b_1 = [SQRT(e_w) - 1]$ (28)

45

It is therefore possible to obtain estimates of the dielectric constants of the solid- (soil) and water-phase components of the material from:

$$(5L_a - 1) = (\sqrt{\varepsilon_s} - 1)\frac{\gamma_d}{G_s \gamma_w} + (\sqrt{\varepsilon_w} - 1)V_w(\%) \tag{29}$$

Alternatively, the expression for the volumetric moisture content can be determined from:

$$V_w(\%) = \frac{(5L_a - 1) - (\sqrt{\varepsilon_s} - 1)\dfrac{\gamma_d}{G_s \gamma_w}}{(\sqrt{\varepsilon_w} - 1)} \tag{30}$$

or

$$V_w(\%) = \frac{\sqrt{K_a} - 1 - (\sqrt{\varepsilon_s} - 1)\dfrac{\gamma_d}{G_s \gamma_w}}{(\sqrt{\varepsilon_w} - 1)} \tag{31}$$

If in equation (31) we use the simplifying assumptions that $e_s = 4$ and $e_w = 81$ then

$$(\sqrt{\varepsilon_s} - 1) = 1 \tag{32}$$

and

$$(\sqrt{\varepsilon_w} - 1) = 1 \tag{33}$$

or

$$V_w(\%) = \frac{\sqrt{K_a} - 1 - \dfrac{\gamma_d}{G_s \gamma_w}}{8} \tag{34}$$

or

$$V_w(\%) = 0.125\sqrt{K_a} - 0.125 - \frac{\gamma_d}{8G_s \gamma_w} \tag{35}$$

The V_s (%) (where V_s (%) = $\gamma_d/G_s\gamma_w$ term) will generally vary within a small range of values (e.g., 60 to 80 percent) for the majority of highway soils compacted to standard/ modified conditions. It should also be noted that since V_s (%) is divided by 8 [i.e., SQRT(e_w) - 1], the contribution of this constant ($\gamma_d/8G_s\gamma_w$) will only vary between 0.06 and 0.10 percent. Thus, for most highway engineering applications, the influence of V_s (%) can be ignored in the TDR analysis by treating it as a constant in the following equation:

$$V_w(\%) = 0.125\sqrt{K_a} - 0.125 - 0.08$$
$$= 0.125\sqrt{K_a} - 0.133 \tag{36}$$

This analysis helps explain literature models of the form V_w = SQRT(K_a), as shown in models 6 and 7 of table 1a.

As derived, this model can only be used for an FHWA TDR probe with a length of 0.203 m. If a different-length probe is used, the derivation would remain the same, except the new probe length would be substituted. In addition, the assumption of a = 0.5 is directly responsible for the SQRT(x), and as shown in table 1b, this assumption has been used by other researchers, as well as for solving (fitting) the value from nonlinear regression studies.

INITIAL ANALYSIS

The apparent length of the TDR response was determined through the Method of Tangents as discussed in Phase I of this study. Using the equation,

$$y = (5L_a - 1) = B_0\frac{\gamma_d}{G_s\gamma_w} + B_1V_w(\%) \tag{37}$$

we performed a linear regression to determine the coefficients B_0 and B_1 for each soil sample. Table 4 summarizes the results of this initial analysis for the predicted values of B_0 and B_1. Based on the relationship between B_i and e_i, the dielectric constant of the soil (e_s) and the dielectric constant of water (e_w) were also computed. In order for this equation to be valid, the dielectric constant values had to be approximately 4.5 and 81, respectively.

The regression analysis shown in table 4 can be observed for each of the 28 individual soil samples evaluated (No. 1-28). In addition, regression analyses were

47

conducted by AASHTO soil type (No. 29-35), major AASHTO soils (coarse versus fine) (No. 36-37), and finally all soils (No. 38).

An initial review of the data revealed that six soils had a negative B_0 coefficient as shown in table 4. This, of course, is a physical impossibility, as the dielectric constant of the soil must be positive. Figures 13 through 15 plot the predicted volumetric moisture versus the laboratory volumetric moisture for all soils (combined) and for coarse and fine-grained soils.

Figure 13 is a plot of all the soil data points. However, when the soils are separated by coarse and fine-grained, certain outliers are visible. These appear to be linear for the soil sample tests. Referring to figure 14, soil sample 831801 has data points with a much higher slope but a similar intercept, which greatly distorts the overall accuracy of the predictive model. In figure 15, soil sample 091803 has data points that are almost parallel to the line of equality, but with a lower intercept. In addition, soil sample 481068 has data points that are almost parallel but above the line of equality. A double asterisk is placed next to the six soils that displayed a significantly different relationship than the other 22 soils noted in table 4.

Table 4. Summary of Results of Initial Analysis.

No.	Sample No.	AASHTO Class	B_0	B_1	Se	R^2	s	w
1	271018	A-1-b	1.47	7.34	0.183	0.85	6.12	69.52
2	271028	A-1-b	1.13	9.76	0.113	0.96	4.55	115.86
3	161010	A-2-4	1.07	9.02	0.267	0.94	4.27	100.41
4	231026	A-2-4	0.87	9.45	0.081	0.99	3.51	109.30
5**	364018	A-2-4	-1.54	17.72	0.113	0.98	0.29	350.58
6	404165	A-2-4	0.84	10.54	0.391	0.87	3.38	133.22
7**	484142	A-2-4	-0.56	12.16	0.171	0.95	0.20	173.10
8	491001	A-2-4	1.15	9.05	0.070	0.99	4.62	101.06
9	493011	A-2-4	0.04	11.48	0.215	0.97	1.08	155.80
10	561007	A-2-4	0.98	9.35	0.133	0.98	3.93	107.13
11**	831801	A-2-4	-2.06	27.66	0.617	0.90	1.13	821.37
12	251002	A-3	1.22	8.86	0.077	0.98	4.91	97.22
13	276251	A-3	1.43	8.17	0.123	0.95	5.89	84.11
14	331001	A-3	0.38	11.25	0.143	0.98	1.90	150.13
15	351122	A-3	1.20	8.64	0.035	0.99	4.85	92.91
16	481122	A-3	0.44	11.28	0.120	0.98	2.08	150.73
17	483739	A-3	1.03	9.13	0.108	0.99	4.10	102.67
18	893015	A-3	1.36	8.04	0.058	0.99	5.58	81.74
19**	091803	A-4	-1.79	9.36	0.170	0.97	0.63	107.41
20	481077	A-4	1.01	8.88	0.073	0.99	4.02	97.62
21	871622	A-4	0.22	10.96	0.102	0.98	1.49	143.10
22	906405	A-4	1.22	9.07	0.106	0.98	4.92	101.45
23**	081053	A-6	-0.79	12.08	0.499	0.70	0.04	171.03
24	460804	A-6	2.08	7.95	0.571	0.73	9.47	80.08
25	501002	A-7-5	1.44	7.32	0.345	0.82	5.97	69.25
26	833802	A-7-5	0.69	9.35	0.528	0.79	2.85	107.18
27	469187	A-7-6	1.22	9.17	0.496	0.74	4.91	103.48
28**	481068	A-7-6	-3.10	17.94	0.380	0.94	4.43	358.69
29	A-1-b	A-1-b	1.43	7.69	0.170	0.89	5.91	75.58
30	A-2-4	A-2-4	1.08	9.83	0.570	0.72	4.33	117.29
31	A-3	A-3	1.11	9.02	0.120	0.96	4.46	100.42
32	A-4	A-4	1.79	6.26	0.380	0.79	7.77	52.66
33	A-6	A-6	0.11	10.80	0.540	0.75	1.24	139.17
34	A-7-5	A-7-5	1.04	8.49	0.450	0.78	4.16	90.13
35	A-7-6	A-7-6	-0.55	14.07	0.610	0.90	0.21	227.09
36	Coarse	Coarse	1.07	9.55	0.420	0.79	4.27	111.20
37	Fine	Fine	0.79	9.90	0.660	0.80	3.22	118.76
38	All soils	All soils	1.01	9.63	0.520	0.80	4.03	113.04

** Six soils that displayed a significantly different relationship than the other 22 soil samples.
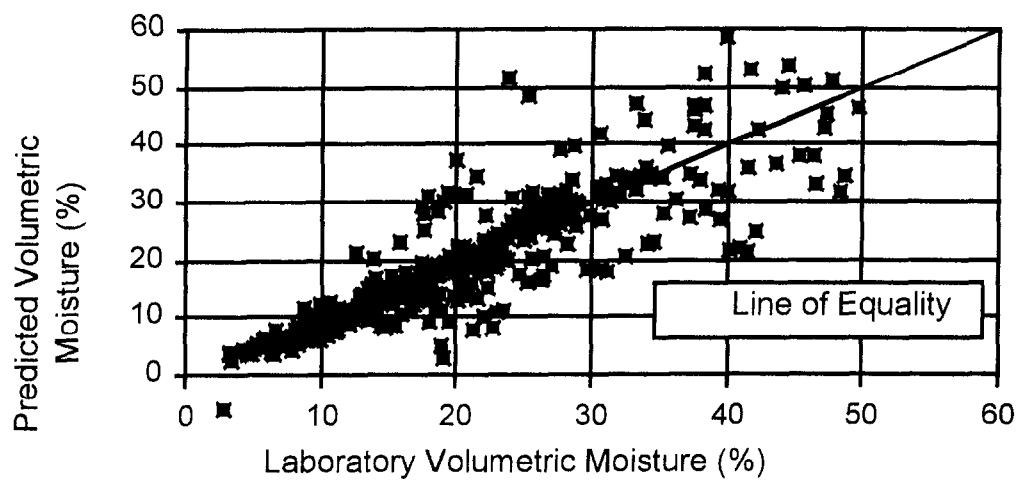
Figure 13. Predicted Volumetric Moisture versus Laboratory Volumetric
Moisture for All Soils.
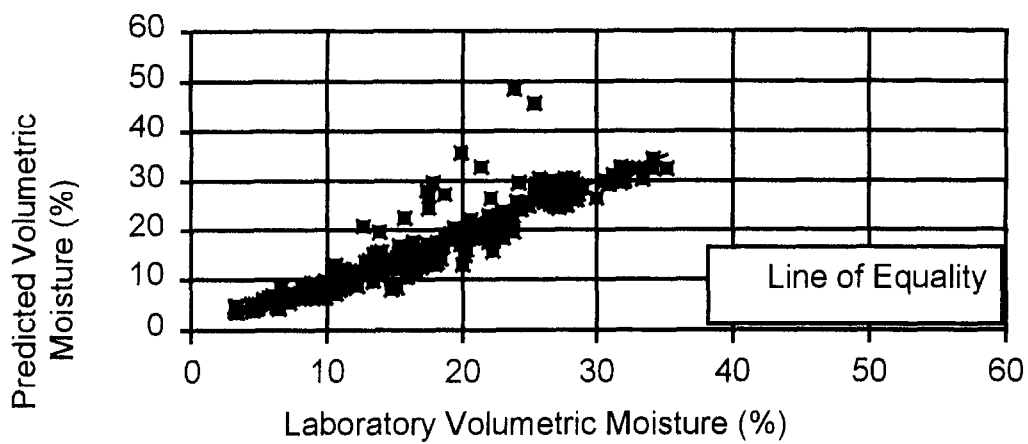
Figure 14. Predicted Volumetric Moisture versus Laboratory Volumetric
Moisture for Coarse Soils.
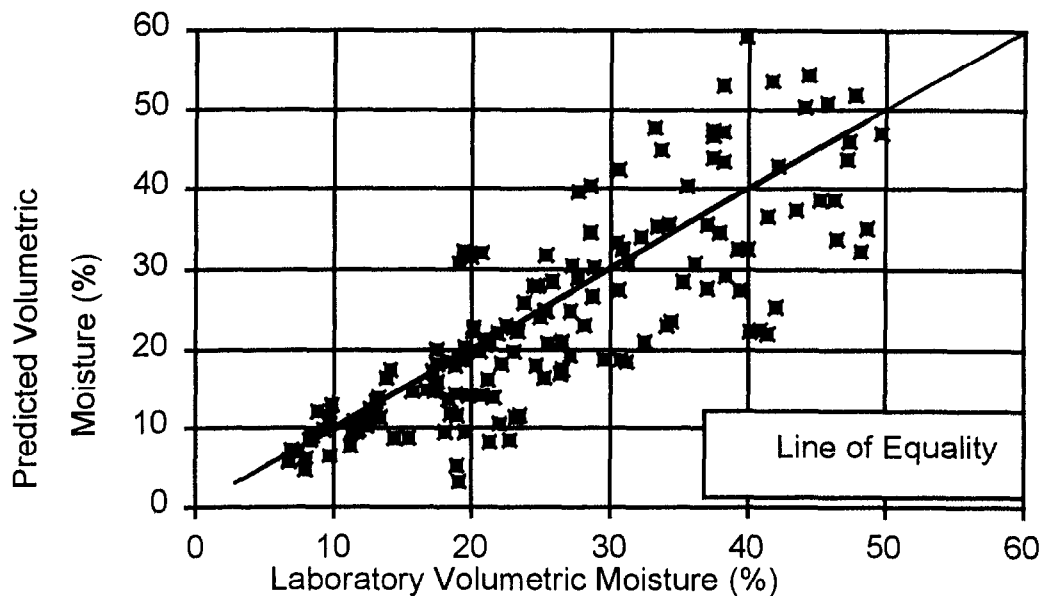
Figure 15. Predicted Volumetric Moisture versus Laboratory Volumetric
Moisture for Fine Soils.

Before these soils were justified as outliers and discarded from further analysis, additional (repeat) laboratory testing was performed to determine if an abnormality in the testing had occurred, or if the soils truly responded with a different calibration curve. This replicate evaluation included testing each of the six questionable soils at two levels of moisture. An additional 54 data points were then added to the previous data. New coefficients (B_0 and B_1) were obtained for each soil sample and the results of the revised analysis are summarized in table 5, with a double asterisk placed by the soils where the coefficients changed.

The original test data compared well to the new test data. For each soil that was retested, the predicted volumetric moisture was plotted against the laboratory volumetric moisture. Although the coefficients of the linear regression changed slightly, the new data were generally consistent with the original data.

It was determined that except for two soils, the retested soils have a different slope than the other data. Soil samples 081053 and 481068 seemed to have a different data

pattern than the original samples. This difference appears to be due to the limitation of the Method of Tangents. These differences occur when the TDR response is shorted and the final inflection point cannot be accurately determined. It was determined that these six soils display different soil properties than the other 22 soils.

Table 5. Summary of Results of Added Data.

No.	Sample No.	AASHTO Class	B_0	B_1	Se	R^2	s	w
1	271018	A-1-b	1.47	7.34	0.18	0.85	6.12	69.52
2	271028	A-1-b	1.13	9.76	0.11	0.96	4.55	115.86
3	161010	A-2-4	1.07	9.02	0.27	0.94	4.27	100.41
4	231026	A-2-4	0.87	9.45	0.08	0.99	3.51	109.30
5**	364018	A-2-4	-1.36	17.34	0.13	0.98	0.13	336.29
6	404165	A-2-4	0.84	10.54	0.39	0.87	3.38	133.22
7**	484142	A-2-4	-0.88	12.90	0.17	0.96	0.02	193.34
8	491001	A-2-4	1.15	9.05	0.07	0.99	4.62	101.06
9	493011	A-2-4	0.04	11.48	0.21	0.97	1.08	155.80
10	561007	A-2-4	0.98	9.35	0.13	0.98	3.93	107.13
11**	831801	A-2-4	-2.23	27.88	0.52	0.90	1.51	834.15
12	251002	A-3	1.22	8.86	0.08	0.98	4.91	97.22
13	276251	A-3	1.43	8.17	0.12	0.95	5.89	84.11
14	331001	A-3	0.38	11.25	0.14	0.98	1.90	150.13
15	351122	A-3	1.20	8.64	0.04	0.99	4.85	92.91
16	481122	A-3	0.44	11.28	0.12	0.98	2.08	150.73
17	483739	A-3	1.03	9.13	0.11	0.99	4.10	102.67
18	893015	A-3	1.36	8.04	0.06	0.99	5.58	81.74
19**	091803	A-4	-2.35	10.08	0.20	0.95	1.82	122.82
20	481077	A-4	1.01	8.88	0.07	0.99	4.02	97.62
21	871622	A-4	0.22	10.96	0.10	0.98	1.49	143.10
22	906405	A-4	1.22	9.07	0.11	0.98	4.92	101.45
23	081053	A-6	-2.24	12.15	0.89	0.67	1.54	173.02
24	460804	A-6	2.08	7.95	0.57	0.73	9.47	80.08
25	501002	A-7-5	1.44	7.32	0.35	0.82	5.97	69.25
26	833802	A-7-5	0.69	9.35	0.53	0.79	2.85	107.18
27**	469187	A-7-6	1.22	9.17	0.50	0.74	4.91	103.48
28**	481068	A-7-6	5.30	5.63	1.28	0.43	39.73	44.01
29**	A-1-b	A-1-b	1.43	7.69	0.17	0.89	5.91	75.58
30**	A-2-4	A-2-4	1.17	9.51	0.55	0.74	4.14	135.46
31**	A-3	A-3	1.11	9.02	0.12	0.96	4.46	100.42
32**	A-4	A-4	1.77	6.25	0.38	0.78	7.66	52.55
33**	A-6	A-6	0.59	9.29	0.80	0.65	2.52	105.88
34**	A-7-5	A-7-5	1.04	8.49	0.45	0.78	4.16	90.13
35**	A-7-6	A-7-6	1.03	10.64	1.03	0.64	4.14	135.46
36**	Coarse	Coarse	1.12	9.40	0.42	0.79	4.48	108.08
37**	Fine	Fine	1.26	8.49	0.77	0.69	5.11	90.12
38**	All soils	All soils	1.33	8.53	0.59	0.74	5.45	90.86

** Soil samples where coefficients B_0 and B_1 were changed.

OUTLIER ANALYSIS

An outlier analysis was conducted to remove suspect data points, such as TDR responses outside its threshold of accuracy. One example, as discussed in the literature review, occurs when the soil is in a saline condition, or the soil is highly conductive. In this case, the final inflection point of the TDR response cannot be accurately determined using the Method of Tangents. Although a logical approximation can be made, the accuracy is highly dependent on the interpreter. To date, little analysis has been conducted to determine the readability of the TDR response when the TDR response is shorted.

Part of the outlier analysis indicated that four soil samples exhibited a shorted TDR response at the higher density levels and/or higher moisture content.

FINAL MODEL DEVELOPMENT

The results used for the final model development did not include the data points where the TDR response appeared to be shorted. Figure 16 contains all the TDR responses of the 28 soil samples, with the deletion of the 39 traces removed by the outlier analysis. Figure 17 contains the coarse soils, and figure 18 contains the fine soils. Overall, each plot shows significant improvement compared to the original plots of figures 13 through 15. In general, the results obtained in this analysis are similar to those obtained from previous research.
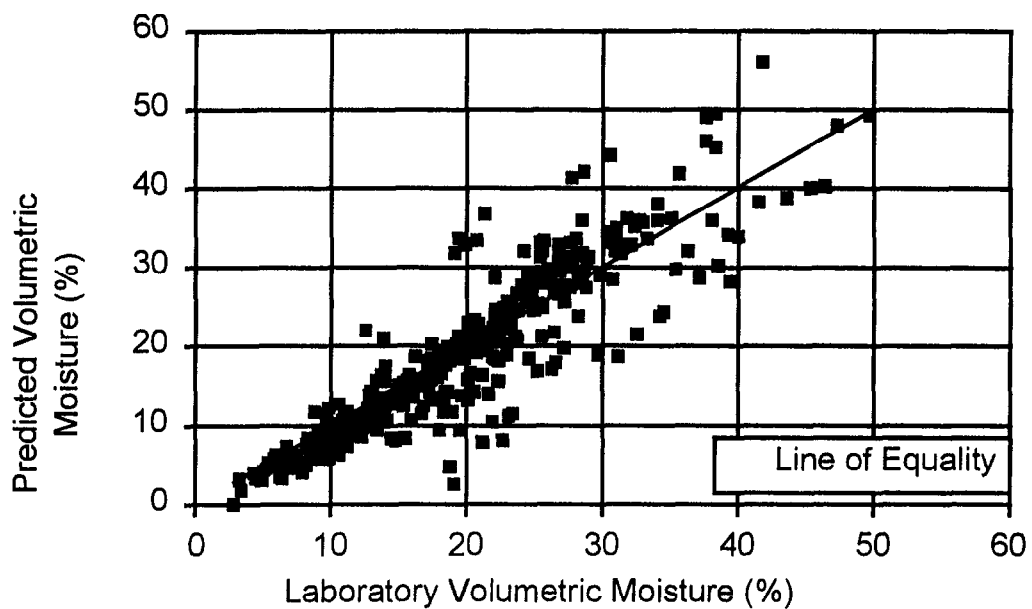
Figure 16. Outliers Removed: Predicted Volumetric Moisture versus
Laboratory Volumetric Moisture for All Soils.
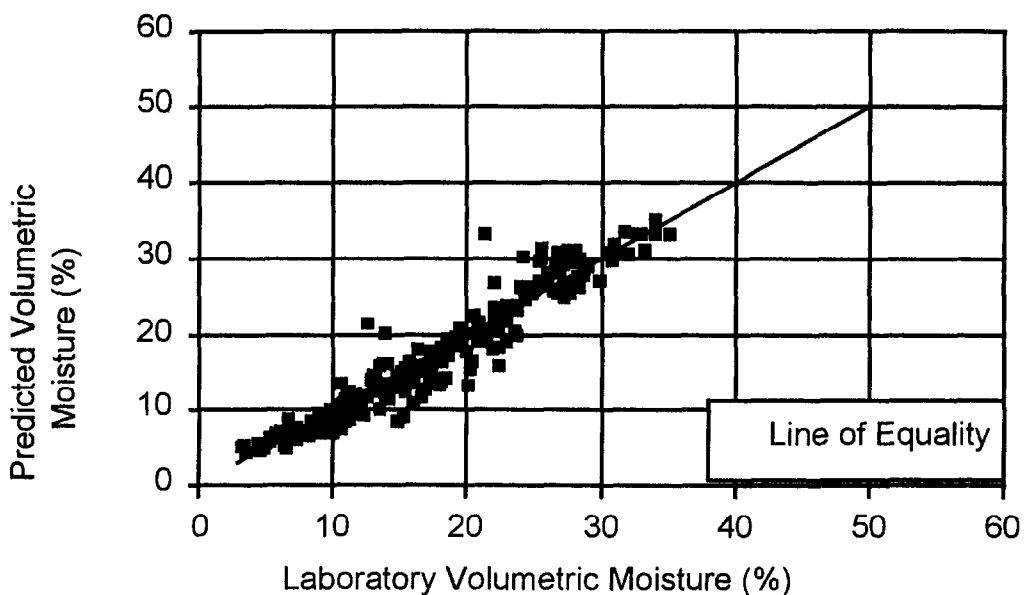
Figure 17. Outliers Removed: Predicted Volumetric Moisture versus
Laboratory Volumetric Moisture for Coarse Soils.
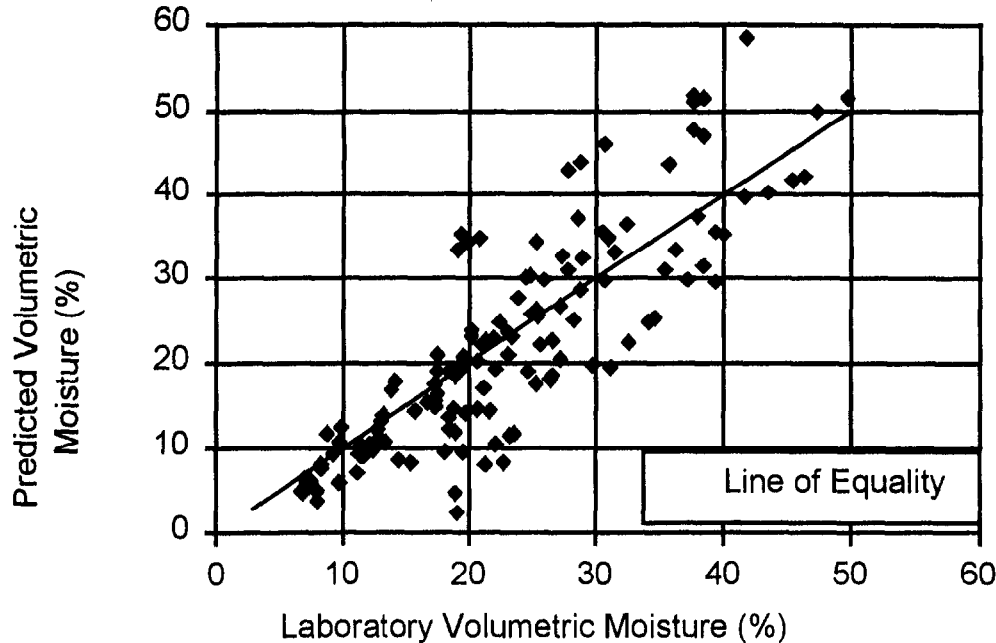
Figure 18. Outliers Removed: Predicted Volumetric Moisture versus
Laboratory Volumetric Moisture for Fine Soils.

A hierarchical methodology for estimating the volumetric moisture content was identified to be best suited for developing a practical implementation scheme for field use. Since the volumetrics of the soil change considerably, it was considered necessary to separate soils by a categorical level. It was decided that one of the optimal and logical approaches would be to base the hierarchical approach on soil type.

As previously noted in this study, the variance and standard error improve considerably as soils are grouped such that the soils have similar volumetric properties. The AASHTO classification groups soils by gradation and Atterburg limits. With these two factors, soils are grouped by similar engineering properties.

The 28 soils tested covered most of the groupings of the AASHTO classification. With these test data, hierarchical levels were defined by: (1) each individual soil; (2) each soil classification; (3) coarse- and fine-grained groups; and (4) all soils grouped together to develop a universal model for all applications.

This approach is recommended, as it is well-suited for determining the volumetric moisture content of a soil in just about any circumstance, from a situation in which no information is known (gradation, Atterburg limits) to a site-specific soil calibration (laboratory analysis necessary). Although site-specific soil calibration would yield the most accurate estimate, a close approximation is all that is needed in many applications. For example, the agricultural community has a need to know when to irrigate their crops in an area that contains similar soils. A universal model can estimate the moisture content within a reasonable limit of accuracy. With a hierarchical model, everyone from generalists to researchers can determine the volumetric moisture content of the soil based on their needs. Each level would use equation 38 to predict the volumetric moisture content.

$$V_w(\%) = \frac{(5 L_a - 1) - B_0 \dfrac{\gamma_d}{G_s \gamma_w}}{B_1} \tag{38}$$

where: L_a = apparent length of the TDR response.

γ_d, γ_w = unit weight of the soil and water.

G_s = specific gravity of the soil.

B_0, B_1 = regression coefficients.

Table 6 shows the results of the hierarchical model developed (level 1-4). Level 4 could determine the volumetric moisture when nothing is known about the soil properties. Equation 39 determines the volumetric moisture content for all soils (universal model).

$$V_w(\%) = \frac{(5 L_a - 1) - 1.41 \dfrac{\gamma_d}{G_s \gamma_w}}{7.98} \tag{39}$$

Figure 16 plots the predicted volumetric moisture versus the laboratory volumetric moisture for all the soil samples tested. The explained variance is 77 percent, with a S_e/S_y equal to 0.59. The standard error of the $V_w(\%)$ is 5.40. The universal model can be used for all soil types when minimal soil properties are known (i.e., estimates of V_s would be necessary).

Table 6. Final Coefficients and Statistics for Mixing Models.

No.	Sample No.	AASHTO Class	B_0	B_1	$(5L_a\text{-}1)$	R^2	V_w (%)	Se/Sy	R^2
1	271018	A-1-b	1.47	7.34	0.18	0.85	2.41	0.49	0.81
2	271028	A-1-b	1.13	9.76	0.11	0.96	1.09	0.21	0.96
3	161010	A-2-4	1.07	9.02	0.27	0.94	2.80	0.27	0.94
4	231026	A-2-4	0.87	9.45	0.08	0.99	0.82	0.11	0.99
5	364018	A-2-4	-1.36	17.34	0.13	0.98	0.75	0.13	0.98
6	404165	A-2-4	0.84	10.54	0.39	0.87	3.50	0.39	0.86
7	484142	A-2-4	-0.88	12.90	0.17	0.96	1.27	0.20	0.96
8	491001	A-2-4	1.15	9.05	0.07	0.99	0.75	0.11	0.99
9	493011	A-2-4	0.04	11.48	0.21	0.97	1.80	0.20	0.97
10	561007	A-2-4	0.98	9.35	0.13	0.98	1.35	0.17	0.97
11	831801	A-2-4	-33.56	36.42	0.42	0.95	1.09	0.20	0.96
12	251002	A-3	1.22	8.86	0.08	0.98	0.83	0.14	0.98
13	276251	A-3	1.43	8.17	0.12	0.95	1.43	0.26	0.94
14	331001	A-3	0.38	11.25	0.14	0.98	1.22	0.16	0.98
15	351122	A-3	1.20	8.64	0.04	0.99	0.39	0.09	0.99
16	481122	A-3	0.44	11.28	0.12	0.98	1.02	0.17	0.97
17	483739	A-3	1.03	9.13	0.11	0.99	1.09	0.10	0.99
18	893015	A-3	1.36	8.04	0.06	0.99	0.70	0.10	0.99
19	091803	A-4	-2.35	10.08	0.20	0.95	1.98	0.23	0.95
20	481077	A-4	1.01	8.88	0.07	0.99	0.79	0.12	0.98
21	871622	A-4	0.22	10.96	0.10	0.98	0.88	0.13	0.98
22	906405	A-4	1.22	9.07	0.11	0.98	1.10	0.15	0.98
23	081053	A-6	NA	NA	NA	NA	NA	NA	NA
24	460804	A-6	2.08	7.95	0.57	0.73	6.87	0.80	0.66
25	501002	A-7-5	1.44	7.32	0.35	0.82	4.57	0.51	0.83
26	833802	A-7-5	0.69	9.35	0.53	0.79	5.48	0.56	0.79
27	469187	A-7-6	1.46	8.23	0.42	0.71	4.99	0.84	0.70
28	481068	A-7-6	27.57	-30.94	0.25	0.74	0.75	0.18	0.96
29	A-1-b	A-1-b	1.43	7.69	0.17	0.89	2.20	0.39	0.87
30	A-2-4	A-2-4	1.00	9.57	0.45	0.81	4.64	0.56	0.78
31	A-3	A-3	1.11	9.02	0.12	0.96	1.35	0.18	0.97
32	A-4	A-4	1.77	6.25	0.38	0.78	6.08	0.55	0.81
33	A-6	A-6	-1.56	12.26	0.75	0.74	5.90	0.63	0.78
34	A-7-5	A-7-5	1.04	8.49	0.45	0.78	5.24	0.56	0.79
35	A-7-6	A-7-6	1.02	10.31	0.53	0.62	5.04	0.92	0.61
36	Coarse	Coarse	1.06	9.30	0.34	0.85	3.65	0.47	0.83
37	Fine	Fine	1.50	7.56	0.54	0.71	7.16	0.70	0.71
38	All soils	All soils	1.41	7.98	0.43	0.78	5.40	0.59	0.77

NA - When outliers were removed, sample size was too small.
Statistics given for Se/R^2 of $(5L_a\text{-}1)$ and Se/R^2 of predicted volumetric moisture.

The Level 3 approach could determine the volumetric moisture when the soil can be identified as either coarse or fine-grained. Equations 40 and 41 determine the volumetric moisture content for coarse and fine grained soils respectively.

$$V_w\ (\%)\ =\ \frac{(5\,L_a\ -\ 1)\ -\ 1.06\dfrac{\gamma_d}{G_s\gamma_w}}{9.30} \tag{40}$$

$$V_w\ (\%)\ =\ \frac{(5\,L_a\ -\ 1)\ -\ 1.50\dfrac{\gamma_d}{G_s\gamma_w}}{7.56} \tag{41}$$

Figures 23 and 24 plot the coarse and fine-grained soils with the outliers removed. The explained variance for the coarse soil is 83 percent, with a Se/Sy equal to 0.47 and a standard error of 3.65. The explained variance for the fine soil is 71 percent, with a Se/Sy of 0.70 and a standard error equal to 7.16. Due to the properties of cohesive soils, it is difficult to estimate the volumetric moisture content of the cohesive soils by either the Level 4 analysis or the fine-grained classification (Level 3 approach). The granular soils (hierarchical Level 3), however, estimate volumetric moisture content significantly better than the Level 4 estimate.

Level 2 is more specific and detailed in that the volumetric moisture content is based on the soil classification, e.g., AASHTO Classification A-2-4. The three soil classifications for which outliers were removed were: A-2-4, A-6, and A-7-6.

Table 6 summarizes the results by AASHTO classification. The classification with the lowest explained variance is A-7-6 with a R^2 equal to 61 percent and a Se/Sy equal to 0.92. These low statistical values are most likely due to the mineralogy or the cohesive nature of the soil.

The most accurate level proposed is Level 1. This approach is based on a site-specific calibrated soil. The soil could undergo laboratory analysis identical to the procedure performed in this study. A calibration curve would be developed using varying moisture levels for each soil for which a volumetric moisture is needed. Once the apparent length of the TDR response is measured, the predicted volumetric moisture can be calculated. Although this procedure is time consuming, the accuracy of the volumetric

moisture is the best estimate produced. The results of each site-specific calibration are tabulated in table 6.

Equation 42 uses this model form with B_0 and B_1 coefficients contained in table 6.

$$V_w(\%) = \frac{(5 L_a - 1) - B_0 \dfrac{\gamma_d}{G_s \gamma_w}}{B_1} \tag{42}$$

Four soil samples contained outliers, which were removed for the final model developed for each soil sample. All such soils, except soil sample #081053, improved substantially. The following briefly summarizes the four soils involved.

Soil sample #831801 increased the explained variance by 6 percent and decreased the standard error by 0.1. Although the statistics are well within acceptable limits, this soil has a negative B_0 coefficient. This coefficient calculates an undefined dielectric constant for the soil. Soil sample #469187 decreased the explained variance by 4 percent, but decreased the standard error by 0.08. Soil sample #481068 increased the explained variance by 31 percent and decreased the standard error by 1.03. For soil sample #081053, a linear regression could not be completed, due to the large number of test results that failed the outlier analysis. The sample originally contained 19 data points, but 15 of the TDR responses appeared to have been shorted. The justification of the shorted TDR response is not completely known, but it would appear that a saline condition was possible.

Regardless of whether Level 1 or Level 4 estimations of the volumetric moisture are used, the results contained in table 6 are the best estimates using the data from this study. There are four soils that have a B_0 coefficient of less than -1.0. Although the regression equation predicts the volumetric moisture content reasonably well, the equations are not "scientifically rational," due to the fact that the dielectric constant of the soil is technically undefined. Further analysis is necessary to determine why these soils do not have similar properties as those of the other soils investigated.

CHAPTER VI: CONCLUSIONS

PHASE I STUDY

Five methods for analyzing the TDR response to determine the apparent length (L_a) were investigated in Phase 1 of this study: Method of Tangents, Method of Peaks, Method of Diverging Lines, Alternate Method of Tangents, and Campbell Scientific Method.

Using 28 soils, we obtained 361 data points from the laboratory analysis previously explained. The results showed that the Method of Tangents appears to be the most accurate procedure for computing the apparent length of the TDR signal response for use in models to predict the volumetric moisture content of soils from measured dielectric values. Using regression models for each method, we conducted a statistical comparison (table 3). The Method of Tangents had an explained variance of 81 percent with a *Se/Sy* of 0.43. These statistics were the best out of the five methods evaluated. The Method of Peaks was second best, with an explained variance of 66.4 percent and a *Se/Sy* equal to 0.58. The least accurate method was the Method of Diverging Lines. This method had an explained variance of 30.7 percent and a *Se/Sy* equal to 0.83.

PHASE II STUDY

Phase II of this study evaluated the parameters affecting the volumetric moisture content of soil, using a regression equation and the mixing model theory. The results of Phase II determined that a hierarchical volumetric moisture predictive methodology is best suited for use with soils of differing mineralogy and physical characteristics. This methodology is applicable when the soils available for study have substantially different volumetric properties, i.e., properties covering the broad range of AASHTO classifications.

This hierarchical methodology includes four levels (1 to 4). Level 4 is a universal model that can be used for any soil type. Level 3 predicts the volumetric moisture content if information is available on whether the soil is coarse or fine-grained. Level 2 can be used if the AASHTO classification is known, whereas Level 1 can be used if the specific soil is calibrated in a laboratory at various levels of moisture. This level would have the highest level of accuracy and the least amount of error in predicting the volumetric moisture content.

In addition to the apparent length obtained from the TDR response, two parameters are required, to account for the volume of the solids. These are: dry density, and the specific gravity of the soil. If the dry density and specific gravity are not known, the volume of the solids can be estimated (since the volume generally varies from 60 percent to 80 percent) for most compacted pavement soils and materials. The volumetric moisture can then be estimated by using the form in equation 43.

$$V_w \; (\%) \; = \; \frac{(5 L_a \; - \; 1) \; - \; B_0 \dfrac{\gamma_d}{G_s \gamma_w}}{B_1} \tag{43}$$

Table 6 in chapter V summarizes the coefficients used in each model, by the hierarchical methodology. A universal model including all 28 soils gives an explained variance of 77 percent with a *Se/Sy* of 0.59. A site-specific model, like soil sample 351122, an A-3 soil, has an explained variance of 99 percent with a *Se/Sy* of 0.09. Overall, the more that is known about a soil's volumetric properties, the more accurately the volumetric moisture content can be predicted. As demonstrated, the *Se/Sy* decreases and the explained variance increases as the hierarchical level changes.

CHAPTER VII: RECOMMENDATIONS

As discussed in the literature review, many other factors are crucial for obtaining even more accurate mixing models than are presented in this study. The factor most needed is more data. Additional soils are needed to fill the gaps in this analysis. The AASHTO classification was used to group the soils in a uniform manner. This initial database is a good foundation, but certain soil classifications have not been tested. Specifically, the AASHTO classification A-5 is not included in this analysis. In addition, there are several classifications that have only a few soil samples for developing the AASHTO classification model. The fine-grained soils, i.e., A-6, A-7-5, and A-7-6, are especially lacking in this area. The granular soils seem not to have as varying effect an that of the fine-grained soils with respect to volumetric moisture content, but more data are needed to verify the results in this study. There were only two soil samples tested in A-1-b and no soil samples for A-1-a. The inclusion of the missing soil samples and the larger sample size should result in better and more accurate models. Additional testing is necessary to complete this database and fine tune the models developed.

A second research priority is studies dealing with the shorting of the TDR probe. Research has found that salinity is the main cause of this condition. Soil mineralogy, however, may also have an influence. Since there is no physical means of extracting the saline condition from the soil, other testing is necessary. In the past, researchers have used frequency domain as a means of estimating the salinity of the soil. Additional research is needed to determine the amount of salinity in the soil mixture and the conductivity of the soil that exhibits the shorting of the TDR response.

Temperature has also been determined to change the dielectric value of soil. Since soil goes through a cycling of temperature, additional research is needed to determine the effects of temperature in a frozen soil with unfrozen water and the effects previous to this state. In addition, there is a need to determine the effects of higher temperatures in the pavement structure on the TDR response.

Additional research is also needed to identify the sensitivity of minerals in the soil. Since soils are made up of a mixture of minerals, the mineralogical breakdown of the soil may be a factor. It is known that minerals have varying dielectric values. This is the basis

for the reasoning that a dry soil has a dielectric value of 3 to 5. The effects of this factor need further research.

The chemical composition of the water affects the dielectric constant, since absorbed (bound) water has a much lower dielectric constant than free pore water. Also, whether the soil is partially saturated or totally saturated will dramatically affect the resultant value of the volumetric moisture content. Additional research is necessary to define better the effects of bound water versus free water.

Although there are many additional parameters that should be investigated, a sound foundation has been established for predicting the volumetric moisture content from three variables: dielectric constant, dry density, and specific gravity. With the inclusion of the additional factors described here, the mixing model developed in this study should increase in accuracy.

REFERENCES

1. Raab, R., Esch, E., and Andrei, R., *Evaluation of a Time Domain Reflectometry Technique for Seasonal Monitoring of Soil Moisture Content Under Road Pavement Test Sections*, SHRP-P-689, June 1994.

2. Topp, G. C., and Davis, A. L., "Time Domain Reflectometry (TDR) and its Application to Irrigation Scheduling," *Advances in Irrigation*, Vol. 3, pp. 107-127, 1985.

3. Paterson, D. E., and Smith, M. W., "The Use of Time Domain Reflectometry for Measurement of Unfrozen Water Content in Frozen Soils," *Cold Region Science Technology*, Vol. 3, pp. 205-210, 1982.

4. Look, B., and Reeves, I., "The Application of Time Domain Reflectometry in Geotechnical Instrumentation," *ASTM Geotechnical Testing Journal*, Sept. 1992.

5. Topp, G. C., Davis, J. L., and Annnan, A. P., "Electromagnetic Determination of Soil Water Content: Measurements in Coaxial Transmission Lines," *Water Resources Research*, Vol. 16, No. 3, pp. 574-582, June 1980.

6. Roth, K., Schulin, R., Fluhler, H., and Attinger, W., "Calibration of Time Domain Reflectometry for Water Content Measurement Using a Composite Dielectric Approach," *Water Resources Research*, Vol. 26, No. 10, pp. 2267-2273, Oct. 1990.

7. Hook, W. R., and Livingston, N. J., *Reducing Propagation Velocity Errors in Time Domain Reflectometry Determinations of Soil Water*, Precision Moisture Instruments, Inc., Canada, 1993.

8. Hook, W. R., and Livingston, N. J., *A Model for the Description and Accuracy Evaluation of Time Domain Reflectometry Measurements of Soil Water*, Precision Moisture Instruments, Inc., Canada, 1993.

9. Esch, D., *Detection of Frozen Soils and Soil Moisture Changes Beneath Highway Pavements*, Alaska Department of Transportation, Headquarters Engineering Standards, Juneau, Alaska, 1994.

10. Patterson, D. E., and Smith, M. W., "The Measurement of Unfrozen Water Content by Time Domain Reflectometry: Results from Laboratory Rests," *Canadian Geotechnical Journal*, Vol. 18, pp. 131-144, 1981.

11. Baker, J. M., and Allmaras, R. R., "System for Automating and Multiplexing Soil Moisture Measurement by Time Domain Reflectometry," *Soil Science Society of America Journal*, Vol. 54, No. 1, pp. 1-6, Jan.-Feb. 1990.

12. Henderson, B., and Turay, S., *Report on Findings Seasonal Testing Instrumentation Pilot GPS 361001 IH 481 5B, E. Syracuse, NY*, Pavement Management Systems Limited, New York, Jan. 15, 1992.

13. Selig, E. T., and Mansukhani, S., "Relationship of Soil Moisture to the Dielectric Property," *Journal of the Geotechnical Engineering Division*, Vol. 101, No. 8, pp. 755-770, Aug. 1975.

14. Henderson, B., Turay, S., and Comstock, S., "Time Domain Reflectometry and Frequency Domain Principles in Estimating Soil Moisture Content," Pavement Management Systems Limited, New York, Working Paper No. 3, 1991.

15. Heimovaara, T. J., and Bouten, W., "A Computer-Controlled 36-Channel Time Domain Reflectometry System for Monitoring Soil Water Contents," *Water Resources Research*, Vol. 26, No. 10, pp. 2311-2316, Oct. 1990.

16. Scott, M. G., Phang, W. A., and Patterson, D. E., *Developments In Situ Monitoring of Moisture in Pavement Structures by Time Domain Reflectometry (TDR)*, The Transportation Technology and Energy Branch, Ontario Ministry of Transportation and Communications, July 1983.

17. Stein, J., and Kane, D. L., "Monitoring the Unfrozen Water Content of Soil and Snow Using Time Domain Reflectometry," *Water Resources Research*, Vol. 19, No. 6, pp. 1573-1584, Dec. 1983.

18. Malicki, M. A., Plagge, R., and Roth, C. H., "Reduction of Soil Matrix Effect on TDR Dielectric Moisture Determination by Accounting for Bulk Density or Porosity," *European Journal of Soil Science*, 1994.

19. Rada, G. R., Elkins, G. E., Henderson, B., Van Sambeek, B., and López, A., Jr., *LTPP Seasonal Monitoring Program: Instrumentation Installation and Data Collection Guidelines*, FHWA-RD-94-110, April 1994.

20. Davis, J. L., and Annan. A. P., "Electromagnetic Detection of Soil Moisture: Progress Report 1," *Canadian Journal of Remote Sensing,* Vol. 3, No. 1, pp. 76-86, 1977.

21. Jacobsen, O. H., and Schjonning, A., "Comparison of TDR Calibration Functions for Soil Water Determination," TDR Symposium, Washington, DC, Sept 16, 1994.

22. Peterson, L. W., "Sampling Volume of TDR Probes Used for Water Content Monitoring: Practical Investigation," TDR Symposium, Washington, DC, Sept. 16, 1994.

23. Knight, J. H., "Sensitivity of Time Domain Measurements to Lateral Variations in Soil Water Content," *Water Resources Research*, Vol. 28, pp. 2345-2352, 1992.

24. Topp, G. C., Zegelin, S. J., and White, I., "Monitoring Soil Water Content Using TDR: An Overview of Process," Symposium and Workshop on Time Domain Reflectometry in Environmental, Infrastructure, and Mining Applications, Evanston, IL, Sept 7-9, 1994.

25. Bliskie, J., Letter for Campbell Scientific, Jan. 4, 1995.

26.   *Handbook of Chemistry and Physics*, 67th ed., CRC Press, Boca Raton, FL., 1986.